



## OPEN PCNA and Rnh1 independently participate in the protection of mitochondrial genome against UV-induced mutagenesis in yeast cells

Martyna Latoszek<sup>1</sup>, Katarzyna Baginska-Drabiuk<sup>1,2</sup>, Ewa Sledziewska-Gojska<sup>1</sup>✉ & Aneta Kaniak-Golik<sup>1</sup>✉

In *Saccharomyces cerevisiae* cells, the bulk of mitochondrial DNA (mtDNA) replication is mediated by the replicative high-fidelity DNA polymerase  $\gamma$ . However, upon UV irradiation low-fidelity translesion polymerases: Pol $\eta$ , Pol $\zeta$  and Rev1, participate in an error-free replicative bypass of UV-induced lesions in mtDNA. We analysed how translesion polymerases could function in mitochondria. We show that, contrary to expectations, yeast PCNA is mitochondrially localized and, upon genotoxic stress, ubiquitinated PCNA can be detected in purified mitochondria. Moreover, the substitution K164R in PCNA leads to an increase of UV-induced point mutations in mtDNA. This UV-dependent effect is highly enhanced in cells in which the Mec1/Rad53/Dun1 checkpoint-dependent deoxynucleotide triphosphate (dNTP) increase in response to DNA damage is blocked and RNase H1 is lacking, suggesting that PCNA plays a role in a replication damage bypass pathway dealing with lesions in multiple ribonucleotides embedded in mtDNA. In addition, our analysis indicates that K164R in PCNA restricts mostly the anti-mutagenic Pol $\eta$  activity on UV-damaged mtDNA, whereas the inhibitory effect on Pol $\zeta$ 's activity is only partial. We also show for the first time that in conditions of dNTP depletion yeast Rnh1 neutralizes deleterious effects of ribonucleotides for mtDNA replication, thereby preventing the enhanced instability of *rho*<sup>+</sup> mitochondrial genomes.

Mitochondrial DNA polymerases  $\gamma$  were long thought to be the only enzymes conferring all DNA synthesis in mitochondria during DNA replication and repair<sup>1–3</sup>. The Poly in budding yeast is a processive single-subunit enzyme endowed with two opposing activities: this of a DNA polymerase and that of a proofreading exonuclease<sup>4</sup>, which is critical for the high-fidelity replication<sup>5</sup>. However, numerous studies have shown that high-fidelity DNA polymerases are prone to replication stalling<sup>6–8</sup>. Stalled replication forks, due to endogenous factors or lesions produced in template DNA by DNA-damaging agents, may result in the generation of deleterious single-stranded DNA (ssDNA) gaps or double-strand DNA breaks (DSBs) which, if unrepaired, lead to a loss of genetic information. Consequently, various molecular mechanisms operate during replication to resolve replication stalling. Those mechanisms can be broadly divided in two modes of fork restart: by a template switch through recombination or by a polymerase switch<sup>9</sup>. In the latter, stalled replication forks are restarted by a polymerase switch from a replicative high-fidelity DNA polymerase to Y-family low-fidelity, exonuclease-devoid, DNA polymerases (in yeast cells: Rad30 [Pol $\eta$ ] or Rev1) that are specialized to replicate across various lesions in template DNA<sup>10,11</sup>. Nucleotide incorporations mediated by Y-family polymerases are usually extended by another exonuclease-devoid, specialized polymerase, polymerase  $\zeta$ , belonging to the B-family of DNA polymerases. Activities exerted by those low-fidelity DNA polymerases, called translesion synthesis (TLS) polymerases, often lead to the generation of mutations in DNA. The TLS pathways are initiated in response to replication stress by mono-ubiquitination of K164 in the replicative sliding clamp<sup>12</sup>, called PCNA (proliferating cell nuclear antigen). PCNA (in *S. cerevisiae* also known as Pol30) in eukaryotic cells is a highly conserved protein forming a homotrimeric complex around DNA. During unperturbed replication, the complex, loaded on DNA at the template-primer junction, functions as a processivity factor for two nuclear replicative polymerases  $\delta$  and  $\epsilon$ <sup>13</sup>. Upon replication stalling, the mono-ubiquitination of K164 in PCNA enables a polymerase switch from the replicative DNA polymerase to a TLS polymerase<sup>14–16</sup>. The mechanism is thought to involve multiple interactions between PCNA, ubiquitin and Y-family TLS polymerases and there is some evidence in a reconstituted setting

<sup>1</sup>Institute of Biochemistry and Biophysics Polish Academy of Sciences, Warsaw, Poland. <sup>2</sup>Present address: Department of Genetics, Maria Skłodowska-Curie National Research Institute of Oncology, Warsaw, Poland. ✉email: esg@ibb.waw.pl; anetak@ibb.waw.pl

for a polymerase exchange dependent on mono-ubiquitinated PCNA<sup>17</sup>. Consequently, the effects of nuclear TLS polymerase activities are dependent on K164 of PCNA<sup>14–16</sup>.

Not much is known about replication stress in yeast mitochondria, but it came as a surprise when two studies showed that three yeast low-fidelity TLS polymerases, Pol $\zeta$  (as a core complex of Rev3 and Rev7), Rev1 and Rad30, were in mitochondria responsible for preventing accumulation of UV-induced point mutations in the mitochondrial 21S rDNA gene, conferring resistance to erythromycin<sup>18,19</sup>. These findings were especially unexpected in the case of Pol $\zeta$  and Rev1, because, firstly, activities of those two TLS polymerases are pro-mutagenic upon UV damage in the nucleus<sup>20</sup>, secondly, spontaneous and UV-induced frameshift mutations in a mitochondrial reporter gene had previously been shown to be mediated, independently, by the same polymerases: Pol $\zeta$  and Rev1<sup>21</sup>. Evidently, the functions of Pol $\zeta$  and Rev1 in mitochondria of UV-irradiated cells are varied and most likely dependent on particular circumstances of replication stress on mtDNA. In contrast, Rad30's anti-mutator function in mitochondria upon UV damage conforms to the polymerase's effect detected in the nucleus under the same genotoxic stress, reflecting the ability of Pol $\eta$  to mediate error-free bypass replication across the most frequent UV lesions in DNA, pyrimidine dimers<sup>10</sup>. Unlike Pol $\zeta$  and Rev1, mitochondrial Rad30's activity limits the occurrence of UV-induced frameshift mutations in mtDNA<sup>19</sup>. The requirement of TLS polymerases for the preservation of the mtDNA wild-type sequence upon UV-induced damage suggests that the TLS polymerases are engaged in the resolution of lesion-induced replication stalling in mitochondria. In an attempt to elucidate this function of TLS polymerases, we show that PCNA is localized to mitochondria in yeast cells and, in this location upon DNA damage, mono-ubiquitinated PCNA is also detected. Furthermore, a strain with the substitution K164R in PCNA exhibits a pronounced defect in the mitochondrial non-mutagenic UV-damage lesion bypass that has previously been shown to be dependent on the three TLS polymerases. The defect is exacerbated in cells lacking the Dun1 kinase whose activity is required for the Mec1/Rad53 checkpoint-dependent dNTP increase in response to DNA damage. The level of mitochondrial point mutations is further synergistically elevated upon inactivation of the *RNH1* gene, coding for dual-targeted RNase H1. RNase H1 is essential for the replication of mtDNA in mammalian cells<sup>22</sup>, but yeast strains lacking Rnh1 do not exhibit significant defects in the maintenance of *rho*<sup>+</sup> mitochondrial genomes<sup>23</sup>. Our results suggest that PCNA plays a role in a lesion bypass pathway dealing with damaged ribonucleotides incorporated in mtDNA. The analysis of strains deleted for genes coding individual TLS polymerases indicate also that K164R in PCNA modulates in the first place the activity of Rad30 and partially that of Rev3 on UV-damaged mtDNA. Finally, we report a synergistically increased spontaneous and UV-induced deficiency of *rho*<sup>+</sup> mtDNA stability in a strain lacking both Rnh1 and Dun1.

## Results

### Pol30 exhibits mitochondrial localization in *S. cerevisiae* cells

To examine whether PCNA is targeted to yeast mitochondria, we used a method, developed originally by Ophry Pines and his collaborators<sup>24</sup>. We constructed a plasmid encoding a fusion protein of Pol30 with the short  $\alpha$  fragment of  $\beta$ -galactosidase attached at the C-terminus. The Pol30- $\alpha$  fusion protein was coproduced in yeast cells with an inactive  $\omega$  fragment of  $\beta$ -galactosidase localized either to the cytoplasm ( $\omega$ c) or mitochondria ( $\omega$ m). As shown in Fig. 1a, in cells producing Pol30- $\alpha$ , the  $\beta$ -galactosidase activity was detected both in the presence of the cytoplasmic  $\omega$  fragment or the mitochondrial one, indicating that Pol30 is a dual targeted protein. To further corroborate the result of the plate assay, we performed a two-step isolation of pure mitochondria from yeast cells. A preparation of crude mitochondria, obtained in a standard cell fractionation method by differential centrifugation, was further purified by ultracentrifugation<sup>25</sup>. Samples of the mitochondria were subsequently tested in a protease protection assay to remove external proteins co-purifying with mitochondria. We also extended the protease assay by an analysis of a mitoplast fraction to establish the distribution of mitochondrial proteins inside mitochondria. The resulting mitochondrial samples were subsequently analysed by western blot with a polyclonal antibody against native yeast PCNA<sup>26</sup>. As shown in Fig. 1b, a small portion of cellular normal-length Pol30 is indeed detected inside the mitochondrial matrix. This is consistent with the result of the  $\alpha$ -complementation assay, because only proteins localized in the mitochondrial matrix can produce positive outcomes in the assay. However, in comparison with the exclusively mitochondrial control protein Cox2, there is a slight decrease of Pol30 in the mitoplast fraction upon protease digestion (fraction VI), suggesting that some mitochondrial Pol30 is also in the intermembrane space and this portion is susceptible to protease digestion. We conclude that Pol30 is detected at low levels inside mitochondria: mostly in the mitochondrial matrix and, partly, also in the intermembrane space. Since polyclonal antibodies are typically heterogeneous, many other protein bands, most likely unrelated to Pol30, were detected in mitochondrial fractions on the blot (Fig. S1a). We corroborated the result in a cell fractionation experiment with a strain carrying the modified *POL30-3HA* gene on the chromosome. The HA-tagged variant of Pol30 was detected inside mitochondria with an antibody against HA (Fig. S1b). Except the tagged Pol30, no other proteins reacting with the anti-HA antibody were detected inside mitochondria. Altogether, our experiments, using two different methods, consistently indicated the unexpected presence of PCNA in yeast mitochondria, at a low, but potentially not negligible, level.

### Ubiquitinated Pol30 is inside mitochondria in response to DNA damage

Attempting to uncover the functional significance of PCNA localization in yeast mitochondria, we considered that one of the possible functions of mitochondrial PCNA was related to a regulation of activities exerted by TLS DNA polymerases in mitochondria upon a genotoxic challenge. Since mono-ubiquitination of PCNA on the conserved K164 promotes the recruitment of TLS polymerases to stalled replication forks in the nucleus<sup>12,14,15</sup>, we tested whether PCNA, in mitochondria purified by ultracentrifugation, was modified by ubiquitination upon DNA damage. For this purpose, we detected ubiquitin PCNA conjugates in lysates of purified mitochondria from cells overproducing His-tagged ubiquitin, using Ni-NTA affinity chromatography under denaturing

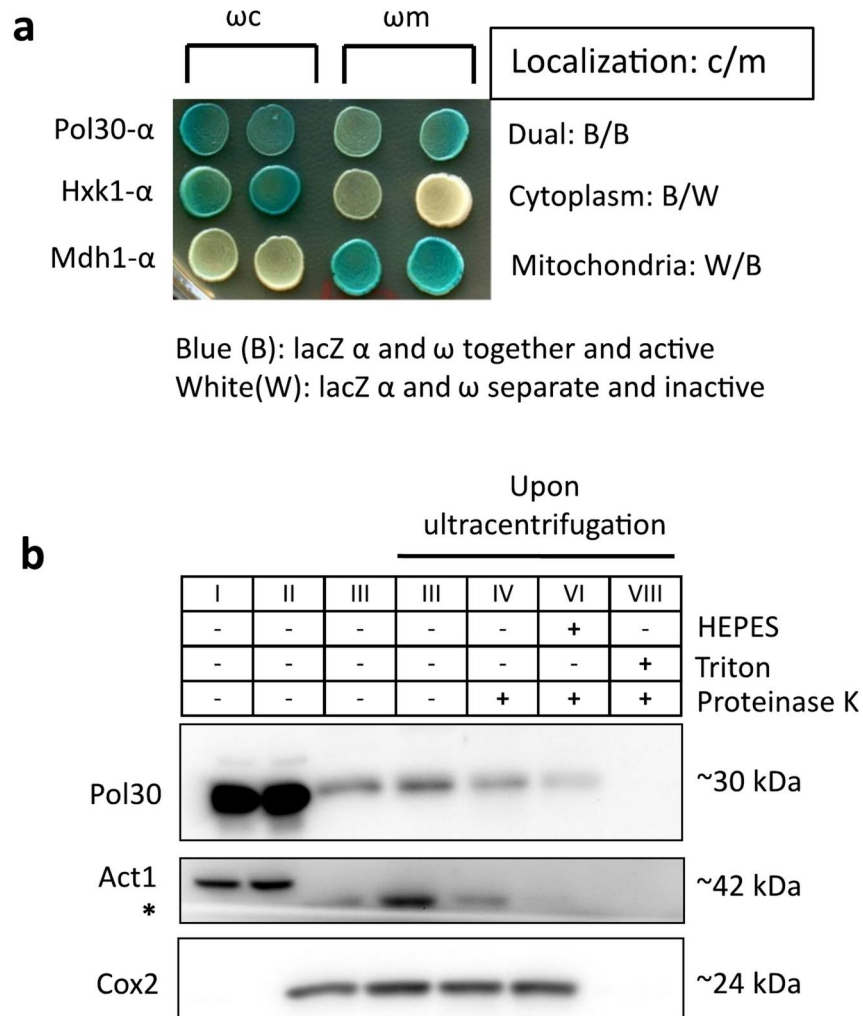


**Fig. 1.** Pol30 is detected in yeast mitochondria. **(a)** Assay of  $\alpha$ -complementation. Cultures of the wild-type strain (FF18733) co-transformed with indicated plasmids encoding Pol30- $\alpha$ , Hxk1- $\alpha$  (cytoplasmic protein control) or Mdh1- $\alpha$  (mitochondrial protein control) and either a plasmid carrying a gene coding the lacZ  $\omega$  fragment localized in the cytoplasm,  $\omega c$  (p877), or a plasmid encoding mitochondrial  $\omega m$  (p999) were spotted on selective synthetic (complete without uracil and leucine) galactose medium plates, buffered with 0.05 M  $KP_i$  at pH 7.0, containing X-gal (5-bromo-4-chloro-3-indolyl  $\beta$ -D-galactopyranoside) at 40 mg/l and incubated for 5 days at 28 °C. Two independent transformant clones for each plasmid pair were tested in parallel for each transformation. Plasmids are listed in Table 2. **(b)** Analysis of fractions from wild-type cells (FF18733) obtained during a two-step fractionation, by differential centrifugation followed by ultracentrifugation, on a western blot. The blot was probed for native Pol30, Act1 (cytosolic control) and Cox2 (mitochondrial control) as described in Methods. Fractions obtained from differential centrifugation procedure—I: total proteins; II: cytosolic proteins; III: mitochondria. Fractions of mitochondria obtained after ultracentrifugation contain the same amount of the mitochondria (50  $\mu$ g) analysed by indicated treatment—III: pure mitochondria; IV: III + proteinase K; VI: III + HEPES + proteinase K; VIII: III + Triton X + proteinase K. The enrichment of the mitochondrial fraction upon ultracentrifugation is  $\sim 250\times$  in comparison to the whole cell and cytoplasmic fraction (in  $OD_{600}$  of cells used for preparation). \* denotes a non-specific signal to the full-length Act1.

conditions<sup>27</sup>. As shown in Fig. 2, unmodified Pol30 was readily detected in resolved protein samples from total cellular extracts of all tested cultures (left panel), however, in diluted mitochondrial lysates, before binding to Ni-NTA resin (middle panel), PCNA was barely visible. In addition to unmodified PCNA, on the blot with total extracts, a weak band of a slower-migrating protein, probably corresponding to mono-ubiquitinated Pol30 ( $\sim 40$  kDa), appeared in the lane with proteins isolated from methyl methanesulfonate (MMS)-treated cells overproducing His-tagged ubiquitin. This conjecture was confirmed by the results of a blot with samples eluted from the Ni-NTA resin upon binding of proteins from mitochondrial lysates (Fig. 2, right panel). Bound ubiquitinated PCNA, mostly mono- and di-ubiquitinated (with very faint bands of Pol30 with possibly more ubiquitin moieties), was detected only in the eluate of proteins from the mitochondrial lysate derived from genotoxin-treated cells overproducing tagged ubiquitin. This result indicates that mitochondrial PCNA is ubiquitinated upon DNA damage and the modified Pol30 may promote TLS in mitochondria as well.

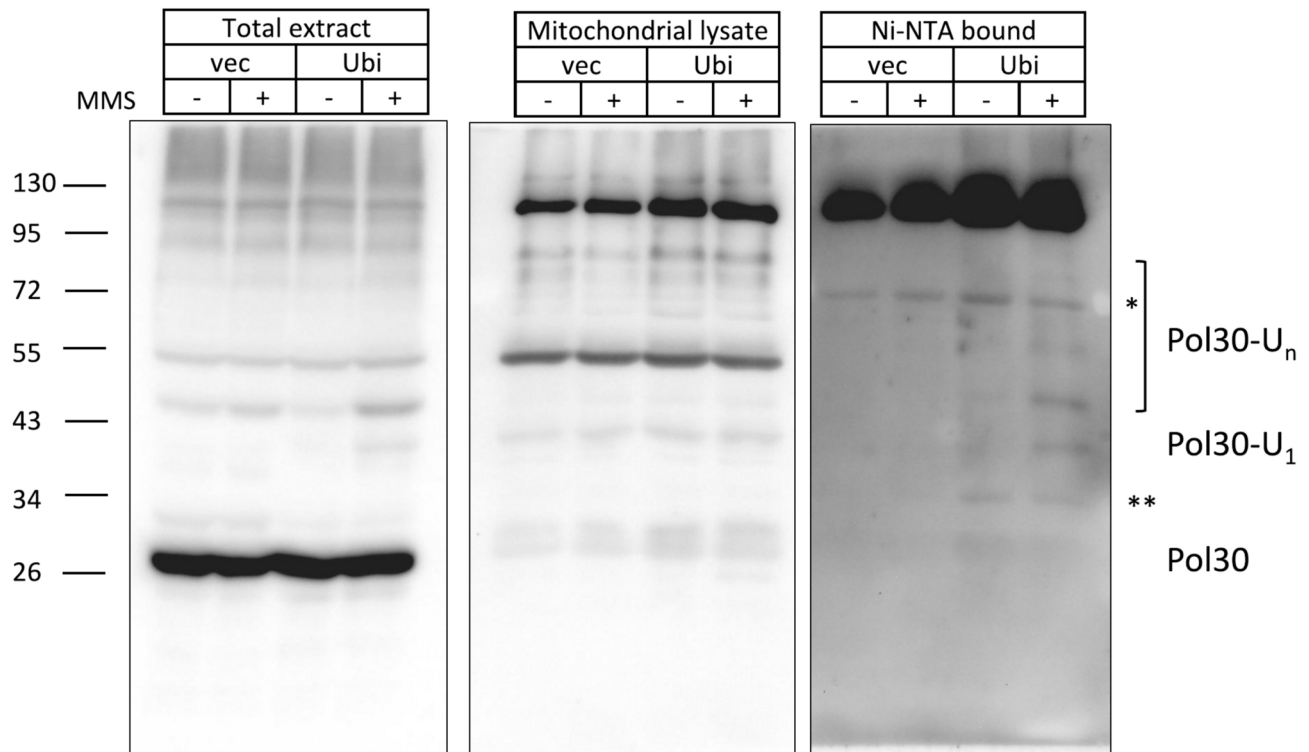


**Fig. 2.** PCNA in mitochondria purified by ultracentrifugation is ubiquitinated upon MMS treatment. Cells of the wild-type strain (FF18733) transformed with pHis-Ub (Table 2) or YEp181 (empty vector) were grown in the presence of 50  $\mu\text{M}$   $\text{CuSO}_4$  and harvested, or treated with 0.05% MMS for 2 h, as indicated. Total cell extracts by TCA precipitation were prepared for western blot according to<sup>60</sup>. Pure mitochondria were solubilized and ubiquitinated proteins from mitochondrial lysates were purified on Ni-NTA beads, as described in Methods. Total, mitochondrial lysate and Ni-NTA-resin bound samples were separated by SDS-PAGE and the resolved proteins were transferred to PVDF membrane overnight, and analyzed with anti-PCNA primary antibodies and anti-rabbit secondary antibodies. Buffers and antibodies are listed in Methods. Symbols: \* and \*\* denote signals that are not specific to ubiquitinated PCNA.

### In response to UV damage, *pol30-K164R* cells accumulate increased numbers of mitochondrial point mutations in a dose-dependent manner

Next we tested the stability of mtDNA upon genotoxic challenge in a strain bearing the *pol30-K164R* allele. The K164R substitution in yeast PCNA precludes its Rad6-dependent mono-ubiquitination<sup>12</sup>, as well as its sumoylation by Siz1<sup>28</sup>. We confirmed in several experiments that the ubiquitination of mitochondrial PCNA, upon MMS- or 4-nitroquinoline 1-oxide (4-NQO)-treatments, was also dependent on K164 (Fig. S2). To test the mitochondrial mutagenesis in the *pol30-K164R* strain and its wild-type counterpart, we used UV as a genotoxic stressor, rather than MMS or 4-NQO, because several previous reports had provided evidence of TLS polymerase activities in yeast mitochondria in response to UV irradiation<sup>18,19,21</sup>. The *pol30-K164R* strain was very sensitive to UV in comparison with the *POL30*<sup>+</sup> reference strain (Fig. 3a), consistently with previous reports<sup>14,15</sup>. In our experiments, we measured two parameters reflecting the stability of mtDNA in *S. cerevisiae* cells: firstly, the frequency of non-respiring (*petite*) cells that arise by frequent rearrangements of mtDNA, and, secondly, the frequency of mitochondrial point mutations conferring resistance to erythromycin. Generation of *petite* mutations and mitochondrial point mutagenesis in yeast cells occur with different frequencies and are due to distinct processes<sup>29</sup>. Those two indicators of mitochondrial genome stability in yeast cells were tested in cultures irradiated by UV doses ranging from 5 to 25 J/m<sup>2</sup>. As shown in Fig. 3b, functional *rho*<sup>+</sup> mitochondrial genomes, necessary for respiration by mitochondria, were increasingly destabilized by rising UV damage. Nonetheless, *petite* frequencies in cultures of both strains at the same UV dose did not differ much. However, an entirely different outcome of UV treatment was uncovered in respect to mitochondrial point mutations in irradiated cultures. Although there was no significant difference between the strains in the accumulation of mitochondrial point mutations in untreated cultures, upon irradiation, even at the lowest UV dose of 5 J/m<sup>2</sup> *pol30-K164R* cultures exhibited a highly significant ( $p < 0.0001$ ) increase of mitochondrial point mutations in relation to their *POL30*<sup>+</sup> counterparts at the same dose (Fig. 3c). With increasing UV doses, frequencies of mitochondrial point mutations in *pol30-K164R* cells increased as well, almost proportionally. We conclude that, in stark contrast to the situation in the nucleus<sup>14</sup>, in the *pol30-K164R* strain UV damage leads to accumulation of mitochondrial point mutations in a dose-dependent manner. Mechanisms counteracting the generation of those UV-induced mutations in yeast mitochondria are thought to encompass the activities of TLS polymerases, Pol $\zeta$ , Rev1 and Rad30<sup>18,19</sup>, though the understanding of their functioning in this location is still insufficient.



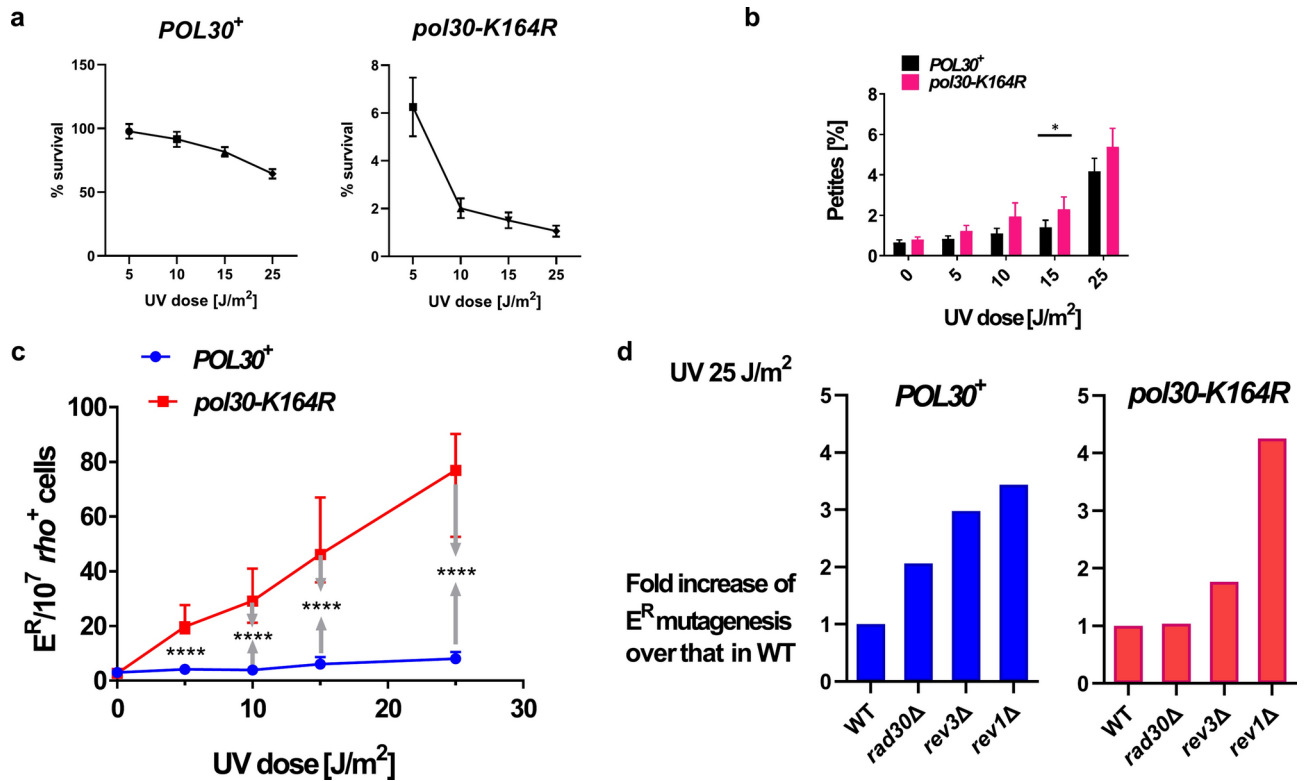


**Fig. 3.** Effect of UV dose on cell survival, occurrence of *petite* mutants and mitochondrial point mutations conferring resistance to erythromycin in the *pol30-K164R* strain compared to those in the *POL30<sup>+</sup>* strain. (a) Average survival [%] of cells in *POL30<sup>+</sup>* (left-hand graph) and *pol30-K164R* (right-hand graph) cultures upon irradiation with indicated doses of UV in relation to untreated cultures. The results are average values  $\pm$  95% confidence intervals of the means from at least 4 independent experiments with 5–10 cultures of each strain. (b) Frequencies of non-respiring (*petite*) mutants in cultures of both strains upon indicated UV dose irradiations. The results are average values  $\pm$  95% confidence intervals of the means from at least 4 independent experiments with 5–10 cultures of each strain. \* denotes *p* value of 0.0489 (Mann–Whitney statistics) for the indicated difference. (c) Frequencies of mitochondrial point mutations ( $E^R$ ) in cultures of the two studied strains upon irradiation with indicated UV doses, after 10 days of incubation at 28 °C. The results plotted are median values from at least 4 independent experiments with 5–10 cultures of each strain and error bars represent 95% confidence intervals of the medians. \*\*\*\* denotes *p* value < 0.0001 (Mann–Whitney statistics). (d) Effects of individual inactivations of three mitochondrial TLS polymerases on UV-induced (at 25  $J/m^2$ )  $E^R$  mutagenesis in the *POL30<sup>+</sup>* and *pol30-K164R* strains. Cultures of the indicated strains were grown and tested as above, but with only one UV dose, and  $E^R$  mutants were scored after 7 days of incubation at 28 °C. Plotted are ratios of median  $E^R$  frequencies in cultures of indicated strains to the median  $E^R$  frequency of the corresponding wild-type control (either *POL30<sup>+</sup>* or the *pol30-K164R* strain). The median values in those ratios are derived from results of 2–6 independent experiments with 10 cultures of each strain. Untransformed values from results of these experiments are shown in Fig. S3. Strains used (in addition to the *POL30<sup>+</sup>* and *pol30-K164R* strains) were: *rad30Δ*: YAK2597 and YAK2598, *rev3Δ*: YAK2651 and YAK2652, *rev1Δ*: YAK2596, *pol30-K164R rad30Δ*: YAK2599, *pol30-K164R rev3Δ*: YAK2653 and YAK2654 and *pol30-K164R rev1Δ*: YAK2803.

### Non-mutagenic bypass activities of Rad30 and Rev3 in mitochondria are deficient upon UV damage in *pol30-K164R* cells

On the basis of the above-described results, we proposed a hypothesis that, under genotoxic challenge, the PCNA-K164R impinging on the functions of TLS polymerases in the mitochondrion. To verify this conjecture, we tested changes in mitochondrial point mutagenesis in UV-irradiated *POL30<sup>+</sup>* and *pol30-K164R* strains lacking individual TLS polymerases. As shown in Fig. 3d (see also Fig. S3), in cells with PCNA-K164R, upon UV irradiation Rad30 no longer contributed to the prevention of induced mitochondrial point mutagenesis and Rev3's contribution was only a fraction of its anti-mutator effect in *POL30<sup>+</sup>* cells. In contrast, the contribution of Rev1 to the anti-mutator mitochondrial activity upon UV damage was surprisingly large (the most substantial of the contributions of the three mitochondrial TLS polymerases), even in *POL30<sup>+</sup>* cells, but it further increased in cells of the mutant strain. These results suggest that the deficiencies of non-mutagenic UV-damage bypass activities of two TLS polymerases, Rad30 and Rev3, in cells with PCNA-K164R may additively account for the observed increases of UV-induced mitochondrial mutagenesis.

## UV-induced mitochondrial mutagenesis is further increased in *pol30-K164R* cells lacking Dun1

The cellular response to replication forks stalling upon encountering damaged DNA template employs two major response pathways: the DNA damage tolerance pathway, acting through the ubiquitination of PCNA<sup>30</sup>, and the global Mec1/Rad53 checkpoint pathway<sup>31</sup>. Each of the two pathways acts in its own specific way to resolve the common activation signal – single-stranded DNA accumulating as a result of replication stress. Although our results strongly suggest that PCNA directly acts in mitochondria in a non-mutagenic lesion bypass engaging translesion polymerases, we addressed also the possibility that the mitochondrial effects in response to UV damage in cells bearing PCNA-K164R may be due to indirect long-range effects emerging from the nucleus to mitochondria under replication stress when the DNA damage tolerance pathways cannot operate properly. We previously reported that increased spontaneous mitochondrial mutagenesis in Rad27- or Rrm3-deficient strains was dependent on Dun1 and increased levels of dNTPs<sup>32</sup>, one of the global responses to replication stress mediated by the Mec1/Rad53-checkpoint pathway. Consistently with the presumption that a defect in DNA damage tolerance might produce an overflow of the activation signal for the DNA damage checkpoint signalling pathway, our results in irradiated *pol30-K164R* cells indicated a prolonged activation of the checkpoint pathway (Fig. S4). This might have an effect on the mutagenesis of mtDNA, as one of the global outcomes of the Mec1 pathway activation, up to eightfold increase in cellular dNTP pools<sup>33</sup>, is Dun1-dependent (reviewed in<sup>34</sup>). Therefore, we examined UV-induced mitochondrial mutagenesis in *pol30-K164R* cells lacking the Dun1 kinase.

Since *DUN1* deletion rendered *pol30-K164R* cells even more sensitive to UV, we could measure UV-induced mitochondrial point mutagenesis in a *pol30-K164R dun1Δ* strain only upon irradiation with the lowest UV dose we tested (5 J/m<sup>2</sup>). The level of mitochondrial point mutations upon UV damage increased synergistically in the *pol30-K164R dun1Δ* strain over the levels detected in both single mutant strains (Fig. 4a), indicating that, strikingly, the checkpoint-mediated increase of dNTPs in irradiated yeast cells was actually required for the non-mutagenic bypass of UV lesions in mtDNA. This result suggests that the elevation of dNTP levels in response to DNA damage is important for the stability of mtDNA. This notion was further supported by inactivating the *SML1* gene in the double mutation strain *pol30-K164R dun1Δ*. When dNTP levels were restored in *pol30-K164R dun1Δ* cells by deleting the *SML1* gene, the frequency of UV-induced mitochondrial mutations decreased

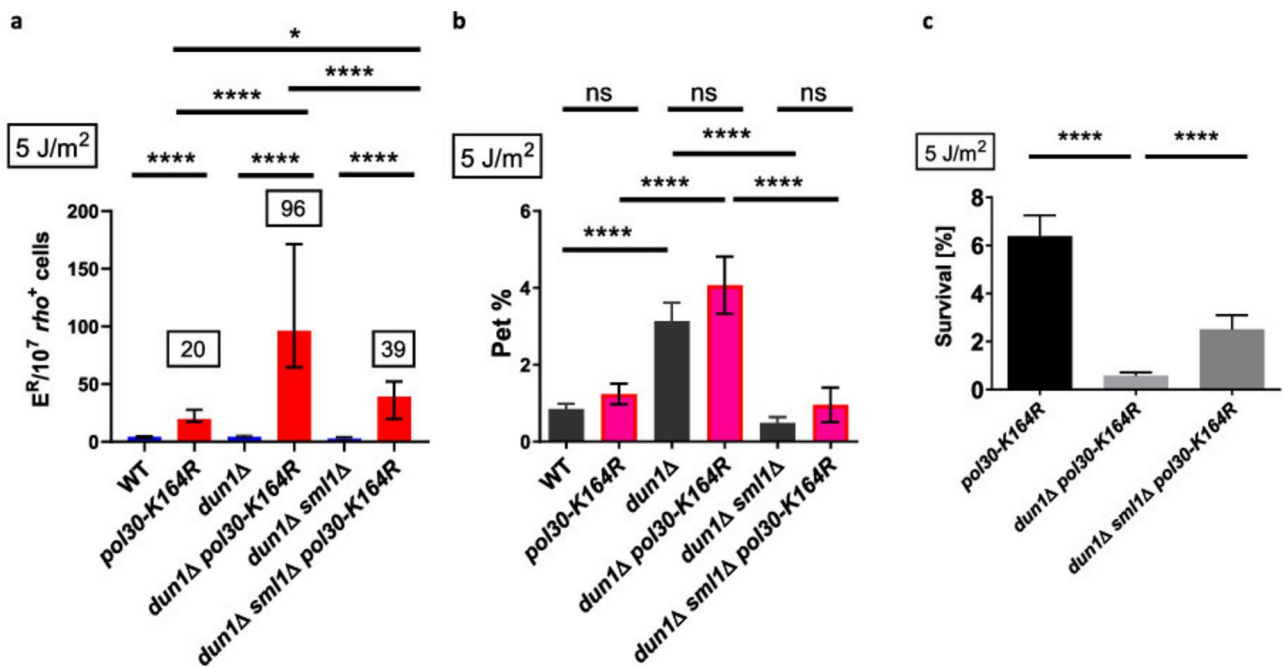


**Fig. 4.** UV-induced mitochondrial mutagenesis is increased in *pol30-K164R* cells lacking Dun1 due to low dNTP levels. Cultures of indicated strains were tested upon irradiation with UV at 5 J/m<sup>2</sup> as described in Methods. **(a)** Frequencies of mitochondrial point mutations (E<sup>R</sup>) upon UV in specified strains. Median values from at least 3 independent experiments with 5–10 cultures of each strain and error bars represent 95% confidence intervals of the medians. \*\*\*\* denotes *p* value < 0.0001, \* denotes *p* value = 0.0261 (Mann–Whitney statistics) for the indicated differences. **(b)** Frequencies of *petite* mutants in cultures of indicated strains upon UV irradiation. The results are average values ± 95% confidence intervals of the means from the same experiments as in (a). \*\*\*\* denotes *p* value < 0.0001 (Mann–Whitney statistics) for the indicated difference. **(c)** Survival ratios [%] in relation to untreated cultures of indicated strains upon UV irradiation at 5 J/m<sup>2</sup>. Average values ± 95% confidence intervals of the means from the same experiments as in (a) and (b). \*\*\*\* denotes *p* value < 0.0001 (Mann–Whitney statistics), “ns”: not significant. Strains used (in addition to the *POL30*<sup>+</sup> and *pol30-K164R* strains) were: *dun1Δ*: YAK3090, *dun1Δ sml1Δ*: YAK3133 and YAK3134, *pol30-K164R dun1Δ*: YAK3091, *pol30-K164R dun1Δ sml1Δ*: YAK3135 and YAK3136.

as well, as had been determined previously<sup>35</sup>, almost to the level of those in the *pol30-K164R DUN1*<sup>+</sup> strain (Fig. 4a). The increase of dNTP levels in the *pol30-K164R dun1Δ* strain, upon *SML1* inactivation, decreased also the level of UV-induced *petite* mutations (Fig. 4b) and partially suppressed the severe sensitivity of *pol30-K164R dun1Δ* cells to UV irradiation (Fig. 4c). We conclude that the major effect of the Dun1 checkpoint-dependent activation, increased dNTP pools, does not account for the enhanced DNA damage-induced mitochondrial mutagenesis in *pol30-K164R* cells. On the contrary, high dNTP levels support the non-mutagenic bypass of UV-caused lesions in mtDNA and are required for the remaining resistance of those cells to UV irradiation.

Consistent with published reports<sup>36,37</sup>, the changes in the overall integrity of *rho*<sup>+</sup> mitochondrial genomes, estimated as frequencies of *petite* mutants, increased in cultures of *dun1Δ* strains (Fig. 4b), indicating the impairment of mechanisms controlling the stability of mitochondrial genomes in cells lacking Dun1. The *dun1Δ* defect of *rho*<sup>+</sup> stability was exacerbated upon UV damage and was entirely dependent on low dNTP pools, because the elevated *petite* generation in *dun1Δ* strains was suppressed upon inactivation of the *SML1* gene. The effect of suppression is also in agreement with a published report by<sup>37</sup>. Similar to the results in Fig. 3, there was no evident difference in *rho*<sup>+</sup> stability between *dun1Δ* cells with either *POL30*<sup>+</sup> or *pol30-K164R* alleles (Fig. 4b). Like in wild-type cells, though in a more pronounced way, in cells devoid of Dun1 the K164R substitution in PCNA specifically affects a mitochondrial pathway mediating the non-mutagenic replication bypass of UV lesions in the mitochondrial 21S rDNA.

### Both overexpression and deletion of *RNH1* influences UV-induced mitochondrial mutagenesis in *pol30-K164R* cells lacking Dun1

Ribonucleotides were detected in the mitochondrial genome of a wild-type yeast strain at a frequency of 1 rNMP per 4500 bp<sup>38</sup>. Apparently, in normal growth conditions this extent of ribonucleotide incorporation into mtDNA is tolerated by the mitochondrial replication and transcription systems. However, in *dun1Δ* cells, in which dNTP pools are maintained at a constitutively low level<sup>35</sup>, it can be expected that ribonucleotide incorporation into mtDNA by the replicative mitochondrial polymerase  $\gamma$  is much more frequent than in wild-type cells. In consequence, it is possible that a part of the elevated UV-induced mitochondrial mutagenesis in *dun1Δ pol30-K164R* cells is connected with the accumulation of rNMPs in the mitochondrial genome. To verify this possibility, we attempted to suppress the UV-dependent mitochondrial mutator phenotype of the *dun1Δ pol30-K164R* strain by overexpressing the *RNH1* gene, coding for yeast RNase H1. Yeast mitochondria lack the system of RNase H2-mediated ribonucleotide excision repair (RER) operating in the nucleus to remove single embedded rNMPs incorporated in the genome during DNA replication<sup>38</sup>. The other ribonuclease targeting ribonucleotides in DNA, RNase H1, is thought to recognize at least four consecutive ribonucleotides in double-stranded DNA (reviewed in<sup>39</sup>). A global study of the *S. cerevisiae* genome has shown that Rnh1 translated starting from the standard AUG does not exhibit a detectable mitochondrial targeting sequence (MTS) according to three mitochondrial targeting prediction programs, but acquires MTS if translated from a non-AUG (near cognate) codon upstream of the canonical AUG<sup>40</sup>—see also Table S1. The mitochondrial localization of the N-extended variant of Rnh1 has been confirmed in the same study. In the current report we further corroborated those findings, using the BiG Mito-Split-GFP assay<sup>41</sup>. We showed that Rnh1-GFP <sub>$\beta_{11ch}$</sub>  translated from the canonical AUG did not enter mitochondria to reconstitute GFP with the mitochondrially encoded GFP <sub>$\beta_{1-10}$</sub>  fragment, but was efficiently targeted to mitochondria when the *RNH1* construct was N-terminally extended <sub>$\beta_{1-10}$</sub>  by 21 codons (Fig. 5), starting with a non-AUG start codon (ACG), as previously proposed<sup>40</sup>. Upon the confirmation of the mitochondrial presence of Rnh1 in yeast cells, we tested effects of Rnh1 overproduction from its gene cloned on a centromeric vector under its native promoter and terminator sequences. It turned out that the centromeric plasmid with the *RNH1* gene did partially suppress the UV-induced mitochondrial mutator phenotype of *dun1Δ pol30-K164R* cells (Fig. 6). The suppressing effect of moderately increased levels of Rnh1 in *dun1Δ pol30-K164R* cells is consistent with the notion that the elevated UV-damage induced mitochondrial mutagenesis in these cells is caused by pro-mutagenic accumulation of multiple embedded ribonucleotides in mtDNA. To further confirm this indication, we next tested a combination of inactivation of *DUN1* and *RNH1* in the context of either *POL30*<sup>+</sup> or *pol30-K164R*.

Our tests showed that inactivation of the *RNH1* gene in the *POL30*<sup>+</sup> strain moderately (by 2.5-fold as  $p < 0.0001$ ) increased spontaneous and UV-induced mitochondrial mutagenesis (Fig. 7a and c). In an *rnh1Δ* strain with the K164R substitution in PCNA the increase of the levels of E<sup>R</sup> mutations detected upon UV was multiplicative, and not additive, over increases in the *pol30-K164R* and the *rnh1Δ* single mutants. This result suggests that UV-induced lesions in mtDNA, which ultimately give rise to E<sup>R</sup> mutations, are either processed in a non-mutagenic way by a pathway dependent on K164 of Pol30 or by Rnh1. This implies that the unknown mitochondrial UV-lesion bypass pathway dependent on K164 of PCNA targets UV-damaged ribonucleotides in yeast mitochondrial genomes. The analysis of mutagenesis in a strain with combined three mutations further strengthens the inference. Introduction of the *pol30-K164R* allele into the *rnh1Δ dun1Δ* strain led to synergistically increased E<sup>R</sup> mutagenesis induced by UV irradiation (Fig. 7b), but not spontaneous mutagenesis (Fig. 7c). In conditions of dNTP depletion, when Dun1 is inactive, it can be expected that more, susceptible to UV-damage, ribonucleotides are incorporated into mtDNA. Since the number of UV-induced mutations in mtDNA in the triple mutant strain increases synergistically, this means that the causative damage cannot be processed in this strain in an error-free way by either a pathway dependent on K164 of PCNA or repaired by Rnh1. Altogether, these findings indicate that K164 of yeast PCNA is needed to curtail mitochondrial mutagenesis induced by UV-damaged ribonucleotides embedded in mtDNA.

Furthermore, underscoring the as-yet unrecognized role of Rnh1 in the repair of mtDNA in yeast cells, we found also a strong synergistic destabilization of *rho*<sup>+</sup> genomes in untreated cultures of the double deletion *rnh1Δ dun1Δ* strain (Fig. 7d). Clearly, the lack of Rnh1 combined with decreased dNTP levels confers also a strong defect in a mitochondrial pathway responsible for the maintenance of the integrity of functional mitochondrial

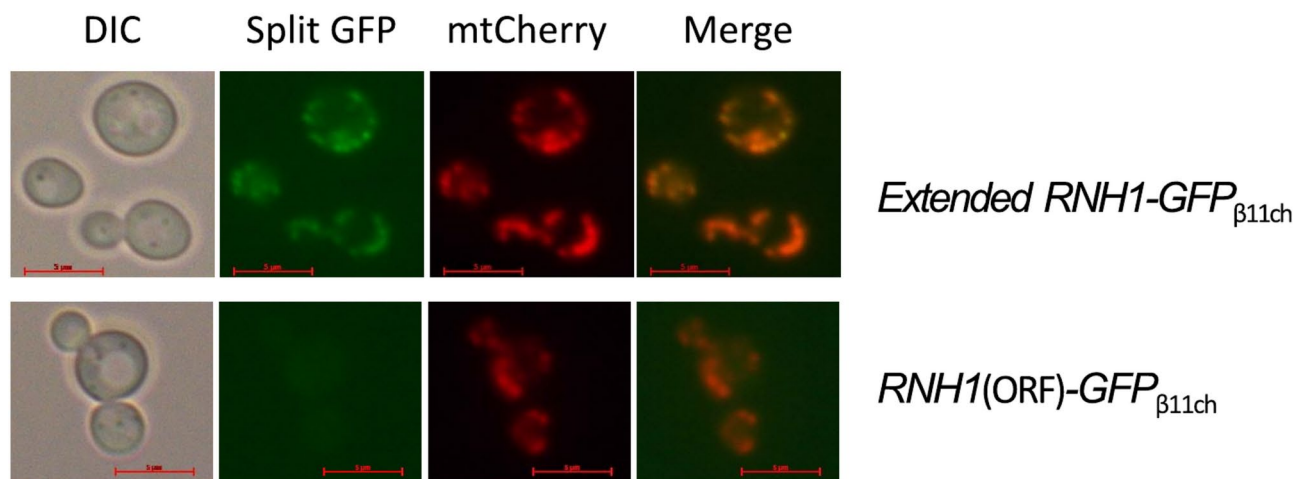


**Fig. 5.** Mitochondrial localization of N-terminally extended Rnh1-GFP<sub>β11ch</sub>. The strain BiG Mito-Split-GFP<sup>41</sup> was transformed with either a plasmid carrying a gene coding for the N-terminally extended Rnh1 fused to GFP<sub>β11ch</sub> (=pCK130) or a plasmid carrying a gene encoding the standard *RNH1* ORF in a fusion with GFP<sub>β11ch</sub> (=pCK131). Those transformant strains expressed also mitochondrial mCherry (from pMW14; Table 2) to stain mitochondrial network in cells. Cells were observed by fluorescence microscopy and by interference differential contrast (DIC) microscopy using an AXIO Observer d1 (Carl Zeiss) epifluorescence microscope with a Zeiss EC Plan-NEOFLUAR 100×/1.3 NA objective, operated by the Zeiss Axio Vision 4.8 software. Scale bar 5 μm.

genomes. To the best of our knowledge, it is for the first time when such a strong phenotype indicating a defect of the stability of *rho*<sup>+</sup> genomes has been described for a yeast strain lacking Rnh1. Loss of functional mtDNA (i.e. *petite* mutation) in yeast cells is usually a consequence of mitochondrial genome rearrangements. Mechanisms responsible for those rearrangements in yeast mitochondria, in spontaneous or genotoxic conditions, are not well understood yet. The synergistic increase in *petite* generation in the *rnh1Δ dun1Δ* strain seems to be largely independent of K164R in PCNA, but cultures of cells with this substitution in Pol30 do tend to exhibit significantly higher *petite* generation levels than *POL30*<sup>+</sup> controls, in particular upon UV irradiation (Fig. 7d). These results suggest that the mitochondrial UV-lesion processing pathway dependent on K164 in PCNA acts in conditions of both dNTP decrease and lack of Rnh1 also to counteract *rho*<sup>+</sup>-destabilizing rearrangements of mtDNA.

## Discussion

PCNA is an essential protein for cell viability. It engages in interactions with many proteins<sup>13</sup> and is known to be involved in numerous cellular processes related to transactions on DNA, though its function as a processivity clamp for nuclear replicative DNA polymerases remains the primary one. So far, there is only one, two-decade old, but largely overlooked, report suggesting the presence of PCNA in mitochondria of fungal cells as determined by cell fractionation<sup>42</sup>. We reproduced the finding in *S. cerevisiae* cells by an improved and more thorough fractionation analysis, detecting on western blots either the native Pol30 or a tagged variant of the protein in mitochondria (Figs. 1b and S1), and, in addition, corroborated this result by a different method using  $\alpha$ -complementation in vivo (Fig. 1a). Altogether, our results show that a small pool of cellular PCNA in yeast cells is localized inside the mitochondrial matrix. We presume that there are two main reasons why the idea of mitochondrial PCNA has not found proponents yet. Firstly, there is no indication that the yeast mitochondrial DNA polymerase, or any mitochondrial Poly from other eukaryotic cells, needs PCNA for its enzymatic activity. Secondly, as shown in Table S1, the N-terminal sequence of yeast PCNA does not possess a clear MTS when analysed by three different programs used for MTS predictions<sup>40</sup>. There is a group of mitochondrial proteins entering the mitochondrion in spite of the apparent lack of a canonical N-terminal MTS. It has been shown for a representative of such MTS-less mitochondrial proteins, Mrp17, that the protein is targeted to mitochondria by dispersed internal motifs corresponding to Tom20-binding domains<sup>43</sup>. Our analysis of the Pol30 amino acid sequence, using the Mitofates program for MTS prediction<sup>44</sup>, identified three potential Tom20-binding motifs in the  $\alpha$ -helical segments of the polypeptide, as shown in Fig. 8, although the program did not categorize yeast PCNA as a mitochondrial protein. It can be, however, proposed that in the vicinity of mitochondria, when PCNA is free of DNA, sequence motifs with affinity to mitochondrial import receptors in the dispersed  $\alpha$ -helices of PCNA facilitate a non-canonical import of PCNA to the organelle. It is also of note in this context that other dual-targeted elapsing mitochondrial proteins that are mentioned in the current study in connection with mitochondrial PCNA: TLS polymerases Rad30 (ref. of mitochondrial localization:<sup>19</sup>) and Rev1 (ref. of mitochondrial localization:<sup>21</sup>), do not possess a clear MTS either (Table S1), indicating that many more MTS-less proteins may enter mitochondria in yeast cells.

The physical presence of PCNA in yeast mitochondria brings up the question of the functional significance of mitochondrial Pol30. Even though the mitochondrial PCNA is not active as a processivity clamp during DNA



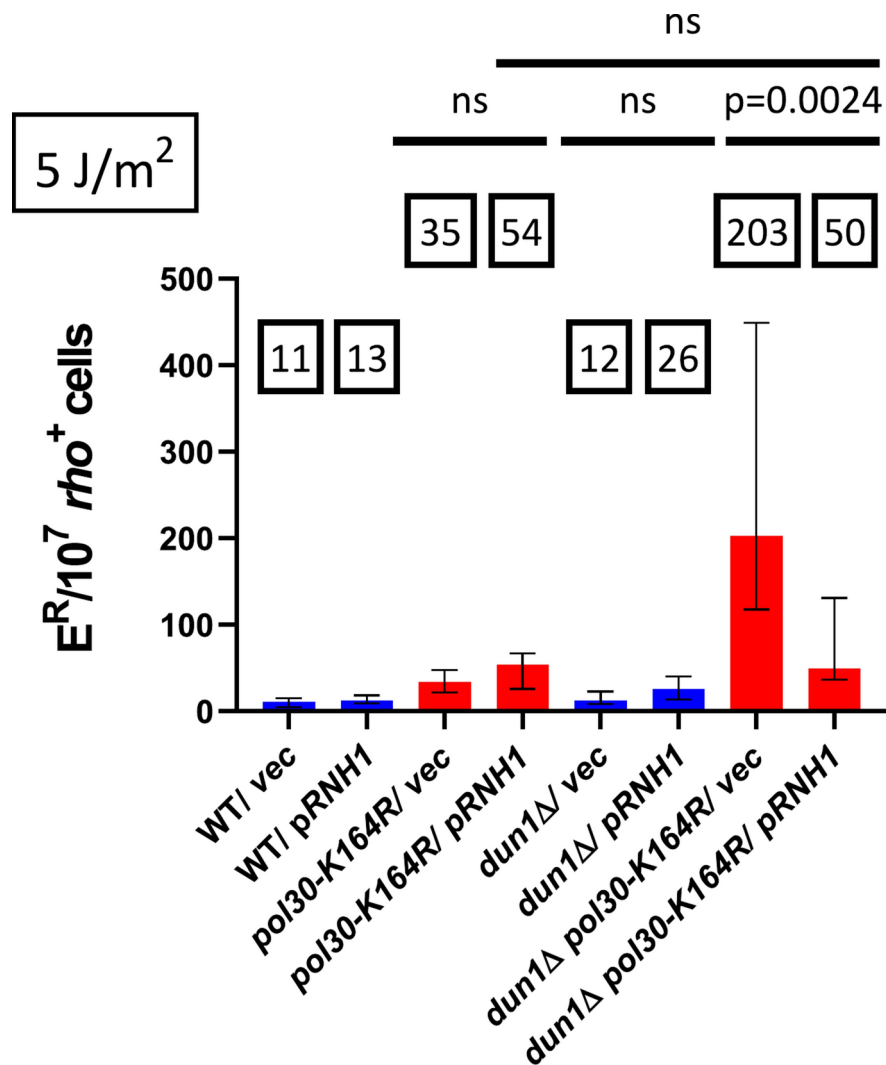


**Fig. 6.** Increased dosage of the *RNH1* gene suppresses the UV-induced mitochondrial point mutator phenotype of the *pol30-K164R dun1 $\Delta$*  strain. Specified strains were transformed with one of the two indicated plasmids – vector: YCplac22 or tested plasmid with the cloned *RNH1*: pRNH1 (= pMW17; Table 2). Single colonies from transformation plates were used to inoculate 3 ml of synthetic complete medium (without tryptophan) with 3% glycerol and 3% ethanol as carbon sources. Cultures were incubated for 2 days at 30 °C and tested in a procedure described in Methods. The graph presents frequencies of mitochondrial point mutations ( $E^R$ ) upon UV at 5 J/m<sup>2</sup> established for indicated transformant cultures. Median values from 2 independent experiments with 10 cultures of each strain and error bars represent 95% confidence intervals of the medians. “ns”: not significant. Strains transformed (in addition to the *POL30*<sup>+</sup> and *pol30-K164R* strains) were the following: *dun1 $\Delta$* : YAK3090, *pol30-K164R dun1 $\Delta$* : YAK3091.

synthesis catalysed by the yeast Poly, a cryptic pool of mitochondrial PCNA may assist in mitochondrial functions of several dual-targeted (nuclear-mitochondrial) proteins that are well-known to physically interact with PCNA in the nucleus: Cdc9, Pif1, Rad27, Ung1 (SGD [<https://www.yeastgenome.org/>] and references therein). Since PCNA is known to be tightly engaged in the DNA mismatch repair reactions in the nucleus<sup>45,46</sup>, there is also a possibility that the eclipsed mitochondrial PCNA operates in the as-yet-poorly-understood pathway/s dependent on the Msh1 protein, a mitochondrial MutS homolog. This MutS-like protein is critically required for the maintenance of the functional mtDNA in yeast cells<sup>47,48</sup>. However, in this first study on mitochondrial PCNA we focused on yet another conceivable function of the mitochondrial DNA clamp: regulation of TLS polymerase activities on damaged mtDNA.

As mentioned in Introduction, yeast mitochondrial low-fidelity TLS polymerases are quite exceptional, because all three of them, Pol $\zeta$ , Rev1 and Rad30 (Pol $\eta$ ), are required for a non-mutagenic bypass of UV-induced lesions in the 21S rDNA gene in mtDNA<sup>18,19</sup>. Since TLS activities in nuclei depend on interactions between Y-family polymerases with the mono-ubiquitinated conserved K164 of PCNA (reviewed in<sup>49</sup>), we first showed that mitochondrial PCNA was indeed ubiquitinated upon DNA damage (Fig. 2). Then, we demonstrated that upon UV irradiation in cells carrying PCNA-K164R more mitochondrial point mutations were generated in a

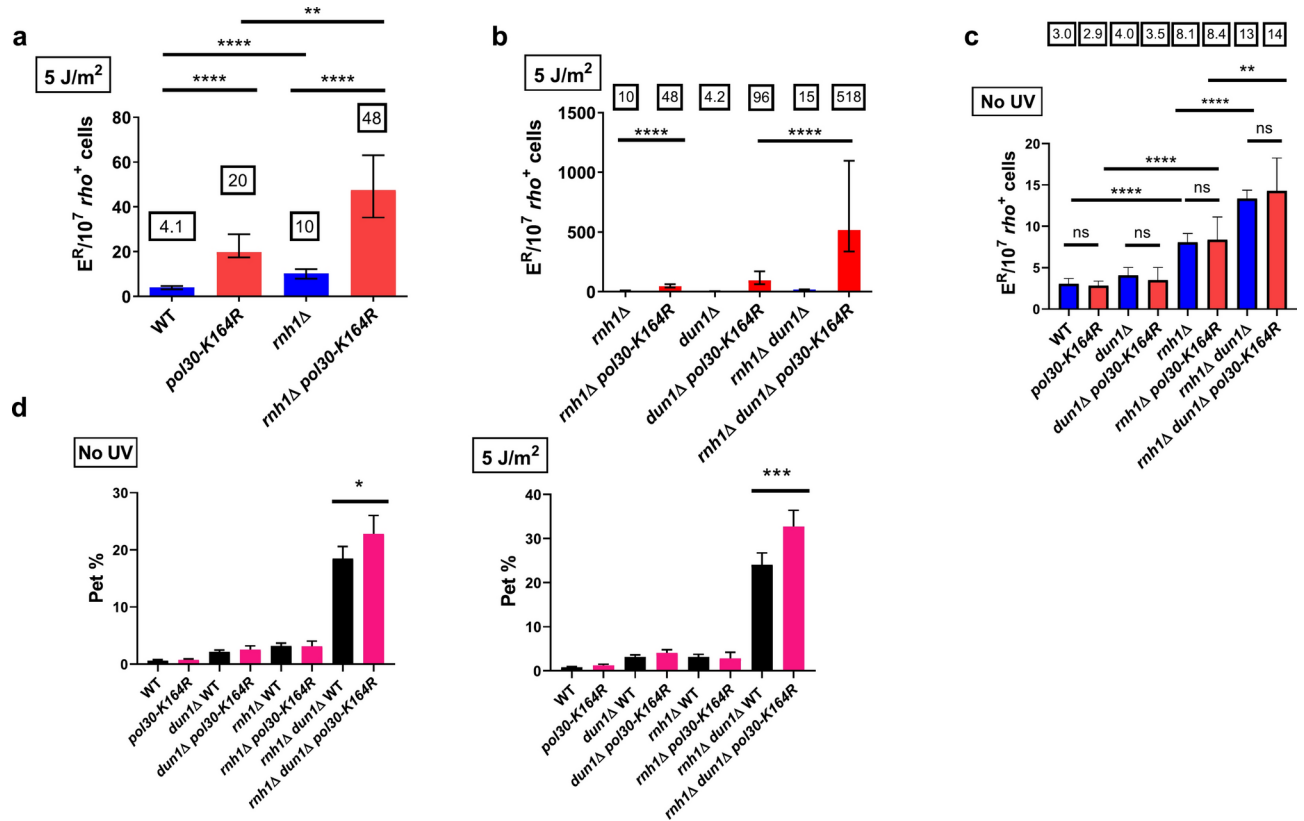


**Fig. 7.** Yeast Rnh1 limits the mitochondrial genome instability resulting from incorporated ribonucleotides in mtDNA. Cultures of indicated strains were inoculated with single colonies (growing on YPD plates for 2–3 days) in liquid YPGE and grown for 2 days with constant agitation. These cultures were tested upon irradiation with UV at 5 J/m<sup>2</sup> as described in Methods. **(a)** Frequencies of UV-induced mitochondrial point mutations (E<sup>R</sup>) upon inactivation of the *RNH1* gene in the *POL30*<sup>+</sup> and *pol30-K164R* strains. Median values from at least 5 independent experiments with 5–10 cultures of each strain and error bars represent 95% confidence intervals of the medians. \*\*\*\* denotes *p* value < 0.0001, \*\* denotes *p* value = 0.0044 (Mann–Whitney statistics) for the indicated differences. **(b)** Frequencies of UV-induced mitochondrial point mutations (E<sup>R</sup>) upon inactivation of the *RNH1* gene in the *POL30*<sup>+</sup> and *pol30-K164R* strains with or without the *DUN1* gene. A continuation of the same analysis as in **(b)**—note a change of scale on the axis Y. Median values from at least 4 independent experiments with 10 cultures of each strain and error bars represent 95% confidence intervals of the medians. \*\*\*\* denotes *p* value < 0.0001 (Mann–Whitney statistics) for the indicated differences. **(c)** Frequencies of spontaneous mitochondrial point mutations (E<sup>R</sup>) upon inactivation of the *RNH1* gene in the *POL30*<sup>+</sup> and *pol30-K164R* strains with or without the *DUN1* gene. Median values from at least 3 independent experiments with 10 cultures of each strain and error bars represent 95% confidence intervals of the medians. \*\*\*\* denotes *p* value < 0.0001, \*\* denotes *p* value = 0.0068, “ns”: non significant (Mann–Whitney statistics). **(d)** Frequencies of *petite* mutants in cultures of indicated strain in spontaneous conditions (the upper graph) or upon UV irradiation (the lower graph). Mean values from at least 2 independent experiments with 10 cultures of each strain and error bars represent 95% confidence intervals of the means. \* denotes *p* value = 0.019, \*\*\* denotes *p* value = 0.0003 (Mann–Whitney statistics) for the indicated differences. Strains used (in addition to the *POL30*<sup>+</sup> and *pol30-K164R* strains) were: *rnh1Δ*: YAK2629, *dun1Δ*: YAK3090, *rnh1Δ dun1Δ*: MW119, *pol30-K164R rnh1Δ*: YAK2630, *pol30-K164R dun1Δ*: YAK3091, *pol30-K164R rnh1Δ dun1Δ*: MW121.

dose-dependent manner than in WT cells, consistent with a defect of the non-mutagenic bypass of UV-induced lesions in mtDNA. These results suggested that PCNA-K164R might affect the activities of mitochondrial TLS polymerases during replication stalling on UV-damaged mtDNA. Our analysis of individual contributions of TLS polymerases to the non-mutagenic bypass in the 21S rDNA locus indicates that mitochondrial TLS polymerases function in at least two distinct pathways preventing UV-induced mitochondrial point mutations. One is dependent on K164 in PCNA and targets mainly Rad30. We presume that this pathway is a canonical TLS pathway mediating replication bypass of UV-lesions in mtDNA. The other mutagenesis-preventing pathway upon UV damage in mtDNA is independent from K164 in PCNA and comprises Rev1 and probably partially Rev3. There were several reports of studies on yeast cells showing TLS activities independent of K164 in PCNA, but the matter is still under debate<sup>49</sup>. However, in higher eukaryotic cells it is already not controversial that TLS polymerases can be active independently of PCNA-Ub<sup>49,50</sup>. Intriguingly, though the activity of Rev1 in preventing UV-induced point mutations does not depend on K164 in PCNA, the elevated contribution of Rev1 does correlate

N-terminus of Pol30: 1-100

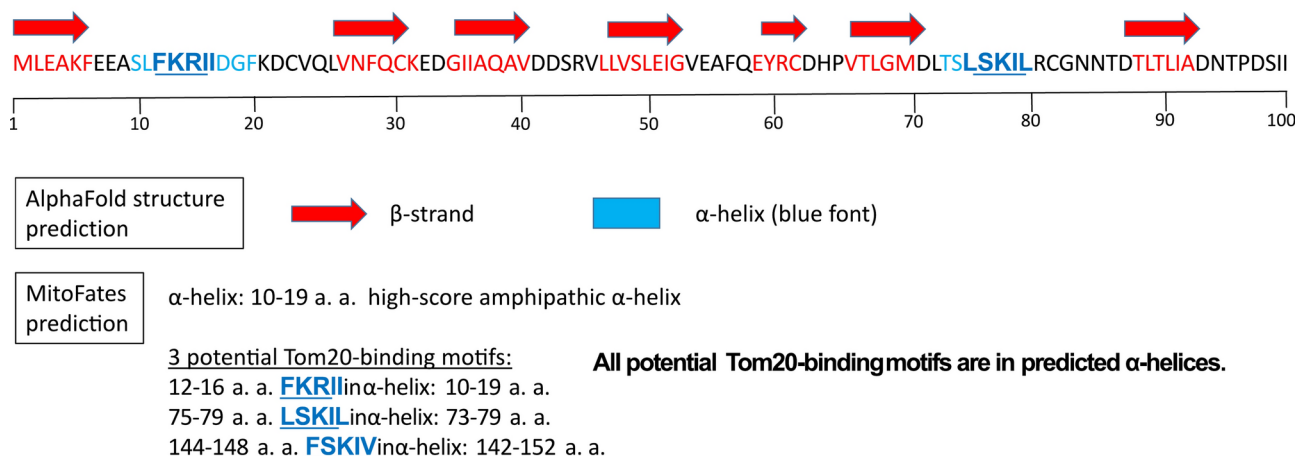


**Fig. 8.** Three Tom20-binding motifs are predicted in  $\alpha$ -helices of yeast Pol30 protein by the MitoFates program using a web server at <http://mitf.cbrc.jp/MitoFates><sup>44</sup>. Only first 100 amino acids (a. a.) are depicted. The secondary structure is according to the AlphaFold Protein Structure Database at <https://alphafold.ebi.ac.uk> and is consistent with the structure described in<sup>61</sup>. Red arrows indicate predicted  $\beta$ -strands. Residues included in  $\alpha$ -helical segments are in blue. Predicted Tom 20-binding motifs are underlined and in bold. The third potential Tom20-binding motif was found by Mitofates when the inquiry had been done with Pol30 without the first 100 amino acids. The structure predicted for amino acids 10–19 is ranked by Mitofates as a high-score amphipathic  $\alpha$ -helix.

with the increased activation of the Mec1/Rad53-checkpoint in UV-irradiated cells carrying PCNA-K164R (Fig. S4). Rev1 has been shown to be phosphorylated in a manner dependent on the Mec1 kinase<sup>51,52</sup>. The elucidation of the non-canonical Rev1-mediated function, we uncovered, on mtDNA will require a thorough analysis of the significance of various domains of this multivalent protein for the mitochondrial function, possible involvement of posttranscriptional modifications, as well as determination of other factors engaging with yeast Rev1 in its mitochondrial activities.

Our results also indicate that, specifically in conditions of dNTP depletion, TLS pathways target UV-damaged ribonucleotides incorporated in mtDNA and, in this task, their function overlaps with that of Rnh1. When those UV lesions cannot be bypassed by the pathways depending on K164 in PCNA, the activity of the mitochondrial RNase H1 is crucial for preventing the generation of mitochondrial point mutations. These results suggest an interpretation that Rnh1 can remove also ribonucleotide tracts containing UV photoproducts. Since yeast strains lacking the ribonuclease have not been shown to exhibit evident mitochondrial defects so far and, in addition, the protein encoded in the standard ORF does not possess a detectable MTS, we have confirmed, using the BiG Mito-Split-GFP assay<sup>41</sup>, the unusual, though not exceptional<sup>40,41</sup>, situation that in yeast cells Rnh1 is a dual targeted protein whose mitochondrial echoform is produced from a non-AUG codon upstream of the canonical ORF. Interestingly, in mammalian cells nuclear and mitochondrial RNase H1 echoforms of divergent abundance are also generated from one mRNA through translation initiation regulation<sup>53</sup>, though the regulatory mechanism is distinctly different from that proposed for the translation of yeast *RNH1* mRNA. In addition, our experiments have revealed that, besides Rnh1's role in the prevention of UV-induced point mutations in mtDNA, the mitochondrial function of Rnh1 becomes critical for the maintenance of *rho*<sup>+</sup> mtDNA in cells with low dNTP levels, suggesting that in these conditions yeast RNase H1 facilitates replication of mtDNA. Future studies should address the elucidation of various transactions engaging this ribonuclease on mtDNA in yeast cells.

## Methods

### Strains and growth conditions

Yeast strains used in the study are listed in Table 1. All deletion allele-bearing strains were made by a PCR-based gene-deletion method, and clones with correct gene inactivations were identified by PCR as described in<sup>32</sup>. The sequences of primers used for generation of deletion cassettes and for verification of gene deletions of indicated genes are listed in Table S2. The following YPD media for growing yeast strains were used: 1% yeast extract (Y; from Difco), 1% peptone (P; Difco), 2% glucose (D). For the purpose of testing mitochondrial mutagenesis in examined strains, cells from single colonies growing on YPD for 2–3 days were inoculated in 3-ml cultures in YP medium containing 0.05 M sodium/potassium (1:4) phosphate, pH 6.2 (after<sup>54</sup>) supplemented with non-fermentable carbon sources: 3% glycerol and 3% ethanol (YPGE). To score non-respiring *petite* mutants, appropriate aliquots of culture dilutions in water were plated on YP medium supplemented with 3% glycerol and limiting 0.1% glucose (YPGd). Plates were incubated for 7 days at 28°C and *petite* and *grande* colonies were scored on each plate. Erythromycin-resistant ( $E^R$ ) mutants were scored, after indicated incubation times, on

Strain	Relevant genotype	Reference
FF18733	<i>MAT</i> leu2-3,112 <i>trp1</i> -289 <i>ura3</i> -52 <i>his</i> -7 <i>lys</i> 1-1	62
POL30 <sup>+</sup>	<i>MAT</i> α <i>his</i> 3-Δ200 <i>leu</i> 2-3,2-112 <i>lys</i> 2-801 <i>trp1</i> -1 <i>ura3</i> -52 <i>pol30</i> Δ::URA3 <i>Y1p128</i> -POL30 <sub>pr</sub> -POL30 <sup>WT</sup> -POL30 <sub>term</sub> -LEU2	14
pol30-K164R	<i>MAT</i> α <i>his</i> 3-Δ200 <i>leu</i> 2-3,2-112 <i>lys</i> 2-801 <i>trp1</i> -1 <i>ura3</i> -52 <i>pol30</i> Δ::URA3 <i>Y1p128</i> -POL30 <sub>pr</sub> -pol30(K164R)-POL30 <sub>term</sub> -LEU2	14
YAK3326	<i>MAT</i> leu2-3,112 <i>trp1</i> -289 <i>ura3</i> -52 <i>his</i> -7 <i>lys</i> 1-1 POL30-3HA-kanMX6	This study (Fig. S1b)
YAK2597	"POL30 <sup>+</sup> " <i>rad30</i> Δ::hphMX	This study
YAK2598	"POL30 <sup>+</sup> " <i>rad30</i> Δ::hphMX	This study
YAK2599	"pol30-K164R" <i>rad30</i> Δ::hphMX	This study
YAK2651	"POL30 <sup>+</sup> " <i>rev3</i> Δ::natMX	This study
YAK2652	"POL30 <sup>+</sup> " <i>rev3</i> Δ::natMX	This study
YAK2653	"pol30-K164R" <i>rev3</i> Δ::natMX	This study
YAK2654	"pol30-K164R" <i>rev3</i> Δ::natMX	This study
YAK2596	"POL30 <sup>+</sup> " <i>rev1</i> Δ::kanMX	This study
YAK2803	"pol30-K164R" <i>rev1</i> Δ::natMX	This study
YAK3090	"POL30 <sup>+</sup> " <i>dun1</i> Δ::kanMX	This study
YAK3091	"pol30-K164R" <i>dun1</i> Δ::kanMX	This study
YAK3133	"POL30 <sup>+</sup> " <i>dun1</i> Δ::kanMX <i>sml1</i> Δ::natMX	This study
YAK3134	"POL30 <sup>+</sup> " <i>dun1</i> Δ::kanMX <i>sml1</i> Δ::natMX	This study
YAK3135	"pol30-K164R" <i>dun1</i> Δ::kanMX <i>sml1</i> Δ::natMX	This study
YAK3136	"pol30-K164R" <i>dun1</i> Δ::kanMX <i>sml1</i> Δ::natMX	This study
YAK2629	"POL30 <sup>+</sup> " <i>rnh1</i> Δ::kanMX	This study
YAK2630	"pol30-K164R" <i>rnh1</i> Δ::kanMX	This study
MW119	"POL30 <sup>+</sup> " <i>dun1</i> Δ::kanMX <i>rnh1</i> Δ::natMX	This study
MW121	"pol30-K164R" <i>dun1</i> Δ::kanMX <i>rnh1</i> Δ::natMX	This study
BiG Mito-Split-GFP	<i>MAT</i> his3-11,15 <i>trp1</i> -1 <i>leu</i> 2-3,112 <i>ura3</i> -1 <i>CAN1</i> <sup>+</sup> <i>arg8</i> ::HIS3	41

**Table 1.** *S. cerevisiae* strains used in this study. "POL30<sup>+</sup>" stands for all the alleles of the strain POL30<sup>+</sup> listed in the 2nd row of the table "pol30-K164R" stands for all the alleles of the strain pol30-K164R listed in the 3rd row of the table.

YP medium with 3% glycerol buffered at pH 6.2 (buffered as above) and containing erythromycin at 4 g/l. To select for the presence of plasmids, synthetic YNB media were used (0.67% Yeast Nitrogen Base from Difco) supplemented with a suitable drop-out mix (for a complete medium, SC, with appropriate omissions) from Bioshop (Bioshop Canada Inc.), according to the manufacturer's instructions, or supplemented with 0.5% casamino acids (to prepare a synthetic complete medium either minus uracil or minus tryptophan), and a carbon source (usually 2% glucose or, for cultures to be tested in mutagenesis assays, 3% glycerol + 3% ethanol). The synthetic media were supplemented, as required, with amino acids or uracil as described previously<sup>32</sup>. Synthetic media with non-fermentable carbon sources were not buffered at pH 6.2 like the YPGE medium.

### Plasmids

*Escherichia coli* strain XL1Blue or JO-FI™ (A&A Biotechnology, Gdansk, Poland) were used for plasmid amplifications and isolations according to standard methods or according to the manufacturer's instructions. Plasmids used or constructed in this study are listed in Table 2. Primers used for described constructions are listed in Table S2. To construct pCK46, p680<sup>55</sup> was linearized with *Pst*I and dephosphorylated. Subsequently, *ACO1* ORF, excluding the stop codon, was replaced by gap repair transformation with *POL30* ORF, excluding the stop codon, amplified with primers OA62 and OA63. To construct pCK129, the *RNH1* gene was amplified with primers FWPstI\_RNH1 and RVEcoRI\_RNH1, on the template of genomic DNA extracted from FF18733, cut with *Pst*I and *Eco*RI and cloned by ligation into the YEplac195 vector<sup>56</sup> cut with the same enzymes. To construct pMW17, the fragment *Pst*I – *Eco*RI with the *RNH1* gene was recombined from pCK129 into YCplac22<sup>56</sup>. To isolate pCK131, pAG416-pGPD-ATP4-GFP<sub>β11ch</sub><sup>41</sup> was cut with *Bam*HI and *Kas*I and closed by a gap repair after co-transformation with a PCR-generated fragment, to replace *ATP4* ORF for *RNH1* ORF (excluding the stop codon) that had been amplified with primers OA514 and OA511. To construct pCK130, pAG416-pGPD-ATP4-GFP<sub>β11ch</sub> was cut with *Bam*HI and *Kas*I and closed by a gap repair after co-transformation with a PCR-generated fragment, that had been amplified with primers OA510 and OA511, to replace *ATP4* ORF for *RNH1* ORF—excluding the stop codon – with the extension of native 63 nucleotides upstream of the start ATG, according to the proposition in<sup>40</sup> for an N-terminal extension of Rnh1 from the alternative translation start at the non-AUG codon (ACG).

### Test of mitochondrial localization by α-complementation

The test was performed as described in<sup>32</sup> and in the legend to Fig. 1a.



Plasmid name	Description	Reference
p680	pRS425-GAL1-ACO1- $\alpha$ (a gift from Ophry Pines)	55
pHXK1- $\alpha$	cytoplasmic protein control (a gift from Ophry Pines)	
pMDH1- $\alpha$	mitochondrial protein control (a gift from Ophry Pines)	
p877	pYES/M15 or pWc (a gift from Ophry Pines)	63
p999	pWm (a gift from Ophry Pines)	63
pCK46	pRS425-GAL1-POL30- $\alpha$	This study
YEplac195	yeast-bacteria shuttle vector, 2 $\mu$ -based with <i>URA3</i>	56
pCK129	YEplac195-RNH1 <sub>pr</sub> -RNH1(ORF)-RNH1 <sub>term</sub>	This study
YCplac22	yeast-bacteria shuttle vector, centromeric with <i>TRP1</i>	56
pMW17	YCplac22-RNH1 <sub>pr</sub> -RNH1(ORF)-RNH1 <sub>term</sub>	This study
YEplac181	yeast-bacteria shuttle vector, 2 $\mu$ -based with <i>LEU2</i>	56
pHis-Ub	YEplac181-CUP1 <sub>pr</sub> -His <sub>7</sub> -Ub (a gift from Ada Skoneczna upon permission from Helle Ulrich)	27
pMW21	<i>TRP1</i> version of YEplac181	This study
pMW22	<i>TRP1</i> version of YEplac181-CUP1 <sub>pr</sub> -His <sub>7</sub> -Ub	This study
pCK132	pCK129 <i>ura3<math>\Delta</math>::TRP1</i>	This study
pMW15	YEplac195 <i>ura3<math>\Delta</math>::TRP1</i>	This study
TTP076	pRS406GPDp-Su9-mCherry (a gift from Maria Bozko upon permission from Brian Zid)	64
pMW14	<i>TRP1</i> version of TTP076	This study
pAG416-pGPD-GFP <sub><math>\beta</math>11ch</sub>	<i>URA3</i> version of the published plasmid (a gift from Róża Kucharczyk)	41
pAG416-pGPD-ATP4-GFP <sub><math>\beta</math>11ch</sub>	ATP4-GFP <sub><math>\beta</math>11ch</sub> construct (a gift from Róża Kucharczyk)	This study
pCK131	pAG416-pGPD-RNH1(ORF)-GFP <sub><math>\beta</math>11ch</sub>	This study
pCK130	pAG416-pGPD-extended-RNH1(ORF)-GFP <sub><math>\beta</math>11ch</sub>	This study

**Table 2.** List of plasmids used in this study with descriptions and references. Primers used for the constructions are listed in Table S2.

### Subcellular fractionation and western blotting

Yeast cells were grown in YPD medium, or as stated, to an OD<sub>600</sub> of 0.8–1 (to harvest cells equivalent to ~800 OD<sub>600</sub>). Mitochondria were isolated according to the protocol for isolation of highly pure mitochondria by ultracentrifugation<sup>25</sup>. After homogenization of zymolyase-treated cells in 30 ml of homogenization buffer (0.6 M sorbitol, 10 mM Tris-HCl, pH 7.4), homogenates were cleared off from cell debris by centrifugation at 1500 g and subsequently at 3000 g for 5 min. Samples of the resulting supernatants, defined as total fractions (fraction I – total, 50  $\mu$ l, corresponding to cell OD<sub>600</sub> of 1.3), were retrieved for analysis by a western blot. Mitochondria were separated from total fractions by centrifugation for 15 min at 12,000 g and supernatants were saved as cytoplasmic fraction (fraction II – cytoplasmic fraction, 50  $\mu$ l) for analysis. Mitochondria were resuspended in SEM buffer (10 mM MOPS/KOH, pH 7.2, 250 mM sucrose, 1 mM EDTA), centrifuged at 3000 g for 5 min and collected again at 12,000 g for 15 min, finally suspended in 1–3 ml of SEM buffer resulting in a crude mitochondrial fraction. To the purification of mitochondria, a sucrose gradient was prepared for each crude mitochondrial suspension in Beckman Ultra-Clear centrifuge tubes, starting with 1.5 ml of ice-cold 60% (w/v) sucrose, then overlaying 4 ml of 32%, 1.5 ml of 23% and 1.5 ml of 15% sucrose, all in EM Buffer (10 mM MOPS/KOH, pH 7.2). Suspensions of crude mitochondria were overlaid on the top of the gradient, tubes were filled with SEM buffer, balanced, and centrifuged in a Beckman SW41 Ti swinging bucket rotor for 1 h at 134,000 g at 4 °C. Pure mitochondria (located at the 32%/60% interface) were collected and centrifuged for 30 min at 10000 g and resuspended in 300  $\mu$ l of SEM buffer.

For Western Blot analysis, pure mitochondria were subjected to submitochondrial fractionation. Firstly, the protein concentration was measured using Pierce Protein Assay (ThermoScientific) and the samples containing 50  $\mu$ g of proteins (in this case, 1/10 of pure mitochondria obtained, corresponding to 80 OD) were further processed. Mitochondria were centrifuged for 10 min in 10000 g and suspended in Laemmli buffer (2% SDS, 10% glycerol, 0.0002% bromophenol blue, 0.0625 M Tris-HCl pH 6.8, 100 mM DTT) and labeled as sample III – pure mitochondria, or processed further. Submitochondrial fractions were prepared by suspending mitochondria in SEM buffer, HEPES buffer (20 mM HEPES-KOH pH 7.4) or Triton buffer (SEM buffer with 1% Triton X-100) and treatment with proteinase K (30  $\mu$ g/ml) for 20 min on ice. Mitoplasts were isolated by treatment of mitochondria with hypotonic HEPES buffer to remove the outer mitochondrial membrane by osmotic rupture. After inactivation of proteinase K with 6 mM PMSF, mitochondria were collected by centrifugation and suspended in 50  $\mu$ l of Laemmli buffer and labeled as samples IV, VI and VIII, respectively). For total and cytoplasmic samples, protein concentration was measured and appropriate volume was mixed with 2 $\times$  Laemmli buffer to obtain protein concentration of 1  $\mu$ g/ $\mu$ l in final samples. All samples were separated by SDS-PAGE and the proteins were transferred to polyvinylidene difluoride (PVDF) membrane (Amersham) overnight. Total and cytoplasmic samples were run at volume corresponding to 0.13 OD, and mitochondrial samples at 32 OD, so final enrichment of mitochondrial samples upon ultracentrifugation is about 250  $\times$ .

Blots were blocked for 1 h in 5% non-fat dry milk in TBST (25 mM Tris-HCl, pH 7.5, 137 mM NaCl, 27 mM KCl, 0.1% Tween-20) before probing with primary antibodies in 1.3% milk in TBST. The following primary

antibodies were used: rabbit polyclonal anti-PCNA (originally from Bruce Stillman; used as in<sup>26</sup> at a dilution of 1:4000), mouse anti-actin monoclonal antibody (Sigma-Aldrich, MAB1501; 1:5000 dilution) or mouse anti-Pgk1 antibody (Abcam, ab113687; 1:10,000 dilution) for the cytoplasmic control and mouse monoclonal anti-MTCO2 (Abcam, ab110271; 1:1000 dilution) or mouse monoclonal anti-porin (Abcam, ab110326; 1:1000 dilution) for the mitochondrial control. After washing with TBST, secondary antibodies were used: polyclonal goat anti-mouse HRP-conjugated Immunoglobulins (Dako, P 0447; 1:2500 dilution) or polyclonal swine anti-rabbit HRP-conjugated Immunoglobulins (Dako, P 0399; 1:3000 dilution). Other western blotting experiments reported in this study were performed essentially as described above or in figure legends. Signals on western blots were detected using a chemiluminescent substrate (Clarity Western ECL substrate, Bio-Rad) for horseradish peroxidase (HRP) using a CCD gel imager.

### Ni-NTA purification of mitochondrial His-tagged Ubiquitin

Cells of the wild-type FF18733 strain (Table 1) were transformed with the plasmid YEplac181-CUP1pr-His-Ubi<sup>27</sup> or the YEplac181 vector<sup>56</sup>. Strains *POL30+* or *pol30-K164R* were transformed with *TRP1*-versions of these two plasmids. The transformants were grown to OD<sub>600</sub> of around 0.8 in the SCGE medium in the presence of 50  $\mu$ M CuSO<sub>4</sub>, and treated with 0.05% MMS for 2 h or 1  $\mu$ g/ml of 4-NQO for 90 min, or further incubated without the genotoxic agent. Mitochondria from cultured cells were purified by ultracentrifugation as described in section Subcellular fractionation and western blotting. Pure mitochondria were solubilized in buffer A (8 M urea, 10 mM NaPi, pH 8.0, 10 mM Tris pH 8.0, 5 mM imidazole, 0.1% Triton X-100, 5 mM  $\beta$ -mercaptoethanol) and a fraction of mitochondrial lysate was saved for western blot. The lysate was incubated with Ni-NTA beads (Ni-NTA Superflow, Qiagen) for 2 h at room temperature with rocking, and washed twice with buffer A, and then twice with buffer B (100 mM NaPi, pH 6.4, 10 mM Tris pH 6.4, 0.1% Triton X-100, 30 mM imidazole, 10 mM  $\beta$ -mercaptoethanol). The proteins bound to the Ni-NTA resin were recovered by boiling in 2 $\times$  Laemmli sample buffer. The total, mitochondrial lysate and Ni-NTA-resin bound samples were separated by SDS-PAGE and the proteins were transferred to PVDF membrane (Amersham) overnight. Western blotting was performed as described above (primary rabbit polyclonal anti-PCNA and secondary polyclonal swine anti-rabbit HRP-conjugated immunoglobulins from Dako).

### Assays of UV-induced mitochondrial mutagenesis

Two standard tests for mitochondrial mutagenesis were used to monitor the maintenance of mtDNA stability in UV-irradiated yeast cells: frequency of *petite* (non-respiring) clones and frequency of erythromycin-resistant mutants. These two divergent types of mtDNA instability in budding yeast cells originate from entirely different molecular mechanisms<sup>57</sup>. On one hand, the relatively frequent occurrence of *petite* (non-respiring) clones is usually due to partial deletions and rearrangements of the mitochondrial genome, leading to a loss of the respiratory function of mitochondria that is dependent on intact mtDNA. Those rearrangements result from prevalent homologous recombination processes in yeast mitochondria that are under an imperfect or limiting surveillance against non-allelic recombination. On the other hand, much less frequent point mutations in the mitochondrial 21S rDNA lead to resistance to erythromycin, an antibiotic targeting the mitochondrial translation apparatus<sup>58</sup>. This mutagenesis depends on various mechanisms shaping the fidelity of mtDNA replication. Spectra of mitochondrial point mutations leading to erythromycin resistance, clustering in two hot spot regions in the mitochondrial gene<sup>59</sup>, have been described in several studies in various genetic contexts<sup>18,32,48</sup>. To test the strains under study, 3 ml-cultures in YPGE medium were inoculated with single colonies growing on YPD plates for 2–3 days and incubated for 2 days at 30 °C with shaking. In case of strains carrying plasmids, the only difference was the medium used for cultures as described in section “Strains and growth conditions”: each culture was inoculated with a single colony growing on selective media upon transformation. To determine cell densities in untreated cultures, cells were diluted in sterile water and appropriate aliquots of dilutions were plated on YPGd plates to obtain around 200–300 colonies per plate. Cells were exposed to specified doses of UV radiation (254 nm) using a UV cross-linker (UVP model CL-1000), within 30 min after plating. Upon UV irradiation and during ensuing incubation, plates were kept in the dark to preclude photo-reactivation. To determine the number of UV-induced E<sup>R</sup> mutants in tested cultures, cells were harvested (from 0.5 ml of a culture) by centrifugation, plated on YPG(pH 6.2) plates with erythromycin and irradiated at an indicated UV dose within 30 min after plating. E<sup>R</sup> mutants were scored after 7 or 10 days of incubation, as indicated, at 28 °C. To determine survival ratios upon UV irradiation and UV-induced numbers of non-respiring mutants, appropriate aliquots of cell dilutions were plated on YPGd plates, then irradiated and incubated for 7 days at 28 °C before scoring *petite* and *grande* colonies. Samples of isolated E<sup>R</sup> mutants in each strain examined in this study were tested by a cytoduction assay to verify the mitochondrial localization of mutations conferring the erythromycin resistance (details of the method available upon request). In the reported experiments in this study, the levels of verified mitochondrial E<sup>R</sup> mutants fell within 90–100%, which is consistent with the notion that mutations conferring erythromycin resistance in *S. cerevisiae* are most frequently localized in mtDNA.

### Data availability

All data necessary for confirming the conclusions of the article are present within the article, figures, tables, supplementary figures (original images to Fig. 1 and 2 are in Fig. S5 and original images to Fig. S1, S2 and S4 are in Fig. S6) and supplementary tables. Strains and plasmids are available from AKG (anetak@ibb.waw.pl) upon request.

Received: 3 July 2024; Accepted: 2 December 2024

Published online: 28 December 2024

## References

- Foury, F. Cloning and sequencing of the nuclear gene MIP1 encoding the catalytic subunit of the yeast mitochondrial DNA polymerase. *J. Biol. Chem.* **264**, 20552–20560 (1989).
- Kaguni, L. S. DNA polymerase  $\gamma$ , the mitochondrial replicase. *Annu. Rev. Biochem.* **73**, 293–320 (2004).
- Copeland, W. C. The mitochondrial DNA polymerase in health and disease, in *Genome Stability and Human Diseases* (ed. Nasheuer, H.-P.) vol. 50 211–222 (Springer, 2010).
- Viikov, K., Jasnovidova, O., Tamm, T. & Sedman, J. C-terminal extension of the yeast mitochondrial DNA polymerase determines the balance between synthesis and degradation. *PLoS ONE* **7**, e33482 (2012).
- Foury, F. & Vanderstraeten, S. Yeast mitochondrial DNA mutators with deficient proofreading exonucleolytic activity. *EMBO J.* **11**, 2717 (1992).
- Khare, V. & Eckert, K. A. The proofreading 3'→5' exonuclease activity of DNA polymerases: a kinetic barrier to translesion DNA synthesis. *Mutat. Res. Mol. Mech. Mutagen.* **510**, 45–54 (2002).
- Zeman, M. K. & Cimprich, K. A. Causes and consequences of replication stress. *Nat. Cell Biol.* **16**, 2–9 (2014).
- Mellor, C., Perez, C. & Sale, J. E. Creation and resolution of non-B-DNA structural impediments during replication. *Crit. Rev. Biochem. Mol. Biol.* **57**, 412–442 (2022).
- Yeeles, J. T. P., Poli, J., Marians, K. J. & Pasero, P. Rescuing stalled or damaged replication forks. *Cold Spring Harb. Perspect. Biol.* **5**, a012815 (2013).
- Prakash, S., Johnson, R. E. & Prakash, L. Eukaryotic translesion synthesis dna polymerases: Specificity of structure and function. *Annu. Rev. Biochem.* **74**, 317–353 (2005).
- Vaisman, A. & Woodgate, R. Translesion DNA polymerases in eukaryotes: What makes them tick?. *Crit. Rev. Biochem. Mol. Biol.* **52**, 274–303 (2017).
- Hoegel, C., Pfander, B., Moldovan, G.-L., Pyrowolakis, G. & Jentsch, S. RAD6-dependent DNA repair is linked to modification of PCNA by ubiquitin and SUMO. *Nature* **419**, 135–141 (2002).
- Moldovan, G.-L., Pfander, B. & Jentsch, S. PCNA, the maestro of the replication fork. *Cell* **129**, 665–679 (2007).
- Stelter, P. & Ulrich, H. D. Control of spontaneous and damage-induced mutagenesis by SUMO and ubiquitin conjugation. *Nature* **425**, 188–191 (2003).
- Haracska, L., Torres-Ramos, C. A., Johnson, R. E., Prakash, S. & Prakash, L. Opposing effects of ubiquitin conjugation and SUMO modification of PCNA on replicational bypass of DNA lesions in *Saccharomyces cerevisiae*. *Mol. Cell Biol.* **24**, 4267–4274 (2004).
- Kannouche, P. L., Wing, J. & Lehmann, A. R. Interaction of human DNA polymerase  $\eta$  with monoubiquitinated PCNA. *Mol. Cell Biol.* **24**, 491–500 (2004).
- Zhuang, Z. et al. Regulation of polymerase exchange between Pol $\eta$  and Pol $\delta$  by monoubiquitination of PCNA and the movement of DNA polymerase holoenzyme. *Proc. Natl. Acad. Sci.* **105**, 5361–5366 (2008).
- Kalifa, L. & Sia, E. A. Analysis of Rev1p and Pol  $\zeta$  in mitochondrial mutagenesis suggests an alternative pathway of damage tolerance. *DNA Repair* **6**, 1732–1739 (2007).
- Chatterjee, N., Pabla, R. & Siede, W. Role of polymerase  $\eta$  in mitochondrial mutagenesis of *Saccharomyces cerevisiae*. *Biochem. Biophys. Res. Commun.* **431**, 270–273 (2013).
- Lawrence, C. The RAD6 DNA repair pathway in *Saccharomyces cerevisiae*: What does it do, and how does it do it?. *BioEssays News Rev. Mol. Cell. Dev. Biol.* **16**, 253–258 (1994).
- Zhang, H., Chatterjee, A. & Singh, K. K. *Saccharomyces cerevisiae* polymerase  $\zeta$  functions in mitochondria. *Genetics* **172**, 2683–2688 (2006).
- Cerritelli, S. M. et al. Failure to produce mitochondrial DNA results in embryonic lethality in Rnaseh1 null mice. *Mol. Cell Biol.* **23**, 807–815 (2003).
- Arudchandran, A. et al. The absence of ribonuclease H1 or H2 alters the sensitivity of *Saccharomyces cerevisiae* to hydroxyurea, caffeine and ethyl methanesulphonate: Implications for roles of RNases H in DNA replication and repair. *Genes Cells* **5**, 789–802 (2000).
- Karniely, S., Rayzner, A., Sass, E. & Pines, O.  $\alpha$ -Complementation as a probe for dual localization of mitochondrial proteins. *Exp. Cell Res.* **312**, 3835–3846 (2006).
- Reinders, J. & Sickmann, A. Proteomics of yeast mitochondria. in *Mitochondria* (eds. Leister, D. & Herrmann, J. M.) vol. 372 543–557 (Humana Press, 2007).
- Krawczyk, M., Halas, A. & Sledziewska-Gojska, E. A novel role for Mms2 in the control of spontaneous mutagenesis and Pol3 abundance. *DNA Repair* **125**, 103484 (2023).
- Davies, A. A. & Ulrich, H. D. Detection of PCNA modifications in *Saccharomyces cerevisiae*. in *DNA Repair Protocols* (ed. Bjergbæk, L.) vol. 920 543–567 (Humana Press, 2012).
- Parker, J. L. et al. SUMO modification of PCNA is controlled by DNA. *EMBO J.* **27**, 2422–2431 (2008).
- Kaniak-Golik, A. & Skoneczna, A. Mitochondria–nucleus network for genome stability. *Free Radic. Biol. Med.* **82**, 73–104 (2015).
- Davies, A. A., Huttner, D., Daigaku, Y., Chen, S. & Ulrich, H. D. Activation of ubiquitin-dependent DNA damage bypass is mediated by replication protein A. *Mol. Cell Biol.* **29**, 625–636 (2008).
- Zou, L. & Elledge, S. J. Sensing DNA damage through ATRIP recognition of RPA-ssDNA complexes. *Science* **300**, 1542–1548 (2003).
- Kaniak-Golik, A., Kuberska, R., Dzierzbicki, P. & Sledziewska-Gojska, E. Activation of Dun1 in response to nuclear DNA instability accounts for the increase in mitochondrial point mutations in Rad27/FEN1 deficient *S. cerevisiae*. *PLoS ONE* **12**, e0180153 (2017).
- Chabes, A. et al. Survival of DNA damage in yeast directly depends on increased dNTP levels allowed by relaxed feedback inhibition of ribonucleotide reductase. *Cell* **112**, 391–401 (2003).
- Williams, L. N. et al. dNTP pool levels modulate mutator phenotypes of error-prone DNA polymerase  $\epsilon$  variants. *Proc. Natl. Acad. Sci.* **112** (2015).
- Gupta, A. et al. Telomere length homeostasis responds to changes in intracellular dNTP pools. *Genetics* **193**, 1095–1105 (2013).
- Fikus, M. U. et al. The product of the DNA damage-inducible gene of *saccharomyces cerevisiae*, DIN7, specifically functions in mitochondria. *Genetics* **154**, 73–81 (2000).
- Zhao, X. & Rothstein, R. The Dun1 checkpoint kinase phosphorylates and regulates the ribonucleotide reductase inhibitor Sml1. *Proc. Natl. Acad. Sci.* **99**, 3746–3751 (2002).
- Wanrooij, P. H. et al. Ribonucleotides incorporated by the yeast mitochondrial DNA polymerase are not repaired. *Proc. Natl. Acad. Sci.* **114**, 12466–12471 (2017).
- Tadokoro, T. & Kanaya, S. Ribonuclease H: molecular diversities, substrate binding domains, and catalytic mechanism of the prokaryotic enzymes. *FEBS J.* **276**, 1482–1493 (2009).
- Monteuuis, G. et al. Non-canonical translation initiation in yeast generates a cryptic pool of mitochondrial proteins. *Nucleic Acids Res.* **47**, 5777–5791 (2019).
- Bader, G. et al. Assigning mitochondrial localization of dual localized proteins using a yeast Bi-Genomic Mitochondrial-Split-GFP. *eLife* **9**, e56649 (2020).
- Laquel-Robert, P. & Castroviejo, M. Stimulation of a mitochondrial endo-exonuclease from *Podospora anserina* by PCNA. *Biochem. Biophys. Res. Commun.* **303**, 713–720 (2003).
- Bykov, Y. S. et al. Widespread use of unconventional targeting signals in mitochondrial ribosome proteins. *EMBO J.* **41**, e109519 (2022).

44. Fukasawa, Y. et al. MitoFates: Improved prediction of mitochondrial targeting sequences and their cleavage sites\*. *Mol. Cell. Proteomics* **14**, 1113–1126 (2015).
45. Pluciennik, A. et al. PCNA function in the activation and strand direction of MutLa endonuclease in mismatch repair. *Proc. Natl. Acad. Sci.* **107**, 16066–16071 (2010).
46. Goellner, E. M. et al. PCNA and Msh2-Msh6 activate an Mlh1-Pms1 endonuclease pathway required for Exo1-independent mismatch repair. *Mol. Cell* **55**, 291–304 (2014).
47. Reenan, R. A. & Kolodner, R. D. Characterization of insertion mutations in the *Saccharomyces cerevisiae* MSH1 and MSH2 genes: evidence for separate mitochondrial and nuclear functions. *Genetics* **132**, 975–985 (1992).
48. Vanderstraeten, S., Van Den Brùle, S., Hu, J. & Foury, F. The role of 3'-5' exonucleolytic proofreading and mismatch repair in yeast mitochondrial DNA error avoidance. *J. Biol. Chem.* **273**, 23690–23697 (1998).
49. Leung, W., Baxley, R. M., Moldovan, G.-L. & Bielinsky, A.-K. Mechanisms of DNA damage tolerance: Post-translational regulation of PCNA. *Genes* **10**, 10 (2018).
50. Paniagua, I. & Jacobs, J. J. L. Freedom to err: The expanding cellular functions of translesion DNA polymerases. *Mol. Cell* **83**, 3608–3621 (2023).
51. Sabbioneda, S., Bortolomai, I., Giannattasio, M., Plevani, P. & Muzi-Falconi, M. Yeast Rev1 is cell cycle regulated, phosphorylated in response to DNA damage and its binding to chromosomes is dependent upon MEC1. *DNA Repair*. **6**, 121–127 (2007).
52. Pagès, V., Santa Maria, S. R., Prakash, L. & Prakash, S. Role of DNA damage-induced replication checkpoint in promoting lesion bypass by translesion synthesis in yeast. *Genes Dev.* **23**, 1438–1449 (2009).
53. Suzuki, Y. et al. An upstream open reading frame and the context of the two AUG codons affect the abundance of mitochondrial and nuclear RNase H1. *Mol. Cell Biol.* **30**, 5123–5134 (2010).
54. Dujardin, G., Pajot, P., Groudinsky, O. & Slonimski, P. P. Long range control circuits within mitochondria and between nucleus and mitochondria: I. Methodology and phenomenology of suppressors. *Mol. Gen. Genet.* **179**, 469–482 (1980).
55. Regev-Rudzi, N., Karniely, S., Ben-Haim, N. N. & Pines, O. Yeast aconitase in two locations and two metabolic pathways: Seeing small amounts is believing. *Mol. Biol. Cell* **16**, 4163–4171 (2005).
56. Gietz, R. D. & Akio, S. New yeast-*Escherichia coli* shuttle vectors constructed with in vitro mutagenized yeast genes lacking six-base pair restriction sites. *Gene* **74**, 527–534 (1988).
57. Kaniak-Golik, A. & Skoneczna, A. Mitochondria-nucleus network for genome stability. *Free Radic. Biol. Med.* **82**, 73–104 (2015).
58. Sor, F. & Fukuhara, H. Identification of two erythromycin resistance mutations in the mitochondrial gene coding for the large ribosomal RNA in yeast. *Nucleic Acids Res.* **10**, 6571–6577 (1982).
59. Sor, F. & Fukuhara, H. Erythromycin and spiramycin resistance mutations of yeast mitochondria: Nature of the rib2 locus in the large ribosomal RNA gene. *Nucleic Acids Res.* **12**, 8313–8318 (1984).
60. Knop, M. et al. Epitope tagging of yeast genes using a PCR-based strategy: More tags and improved practical routines. *Yeast* **15**, 963–972 (1999).
61. Kelman, Z. & O'Donnell, M. Structural and functional similarities of prokaryotic and eukaryotic DNA polymerase sliding clamps. *Nucleic Acids Res.* **23**, 3613–3620 (1995).
62. Aboussekhra, A., Chanet, R., Adjiri, A. & Fabre, F. Semidominant suppressors of Srs2 helicase mutations of *Saccharomyces cerevisiae* Map in the *RAD51* gene, whose sequence predicts a protein with similarities to prokaryotic RecA proteins. *Mol. Cell. Biol.* **12**, 3224–3234 (1992).
63. Dinur-Mills, M., Tal, M. & Pines, O. Dual targeted mitochondrial proteins are characterized by lower MTS parameters and total net charge. *PLoS ONE* **3**, e2161 (2008).
64. Tsuboi, T. et al. Mitochondrial volume fraction and translation duration impact mitochondrial mRNA localization and protein synthesis. *eLife* **9**, e57814 (2020).

## Acknowledgements

We are very grateful for plasmids and/or strains or other reagents to: Bruce Stillman, Helle Ulrich, Paul Kaufman, Ophry Pines, Brian Zid and Roza Kucharczyk. We would like to pass our thanks for help and discussions to our colleagues: Roza Kucharczyk, Maria Bozko, Michal Swirski, Lukasz Borowski, Joanna Kufel, Jakub Piatkowski, Joanna Rusecka, Katarzyna Tonska, Ada Skoneczna and Tuguldur Enkhbaatar. This work was supported by the grant 2017/25/B/NZ3/01,811 (to AKG) from the National Science Center (<https://www.ncn.gov.pl/>) in Poland and by the Institute of Biochemistry and Biophysics PAS Internal grant FBW MG-1/21-15 (to AKG). The funders had no role in study design, data collection and interpretation, or the decision to submit the work for publication.

## Author contributions

ESG and AKG contributed to the conception and design of the work. ML, KBD and AKG constructed all strains and plasmids used in the study and performed all reported mitochondrial mutagenesis tests. AKG performed the alpha complementation experiment. ML performed all fractionation and ubiquitination experiments. ML and AKG performed the BiG Mito-Split GFP assay with *RNH1* plasmids. AKG, ML, KBD and ESG analysed the data. AKG and ESG acquired funding and co-wrote the manuscript with substantive contributions by ML.

## Competing interests

The authors declare no competing interests.

## Additional information

**Supplementary Information** The online version contains supplementary material available at <https://doi.org/10.1038/s41598-024-82104-4>.

**Correspondence** and requests for materials should be addressed to E.S.-G. or A.K.-G.

**Reprints and permissions information** is available at [www.nature.com/reprints](http://www.nature.com/reprints).

**Publisher's note** Springer Nature remains neutral with regard to jurisdictional claims in published maps and institutional affiliations.



**Open Access** This article is licensed under a Creative Commons Attribution-NonCommercial-NoDerivatives 4.0 International License, which permits any non-commercial use, sharing, distribution and reproduction in any medium or format, as long as you give appropriate credit to the original author(s) and the source, provide a link to the Creative Commons licence, and indicate if you modified the licensed material. You do not have permission under this licence to share adapted material derived from this article or parts of it. The images or other third party material in this article are included in the article's Creative Commons licence, unless indicated otherwise in a credit line to the material. If material is not included in the article's Creative Commons licence and your intended use is not permitted by statutory regulation or exceeds the permitted use, you will need to obtain permission directly from the copyright holder. To view a copy of this licence, visit <http://creativecommons.org/licenses/by-nc-nd/4.0/>.

© The Author(s) 2024